Design of Three-Dimensional Digital Filters Using Two-Dimensional Rotated Filters

MICHAEL E. ZERVAKIS, STUDENT MEMBER, IEEE, AND
ANASTASIOS N. VENETSANOPOULOS, SENIOR MEMBER, IEEE

Abstract—**Two techniques for the design of three-dimensional (3-D) filters are introduced in this paper. The first one is based on coefficient transformations of two-dimensional (2-D) circularly symmetric filters. These filters can be designed by cascading 2-D rotated filters. Stability of the 3-D filters designed is discussed and a stabilization procedure based on cepstrum analysis, is proposed. Stable implementation schemes are introduced. The second technique is based on cascade arrangements of 2-D rotated filters and results in 3-D spherically symmetric filters. Examples of 3-D filters designed on the basis of both techniques introduced are presented. Finally, some comparisons among several 3-D design techniques are given.**

INTRODUCTION

THREE-DIMENSIONAL (3-D) image processing has recently emerged as an essential tool in many areas of current interest. This is due to the increasing importance of many applications, where it plays a significant role, and the availability of high-speed computers with large memory. 3-D signals offer significant advantages over 2-D signals, because they preserve spatial information. Depth, surface orientation or edges can be easily detected from 3-D data.

The most important applications of 3-D image processing are the following [1]:

1) *Biomedicine:* 3-D CAT, which has the ability to preserve structures, finds applications in craniofacial surgical planning, the study of the central nervous system, stereostatic neurosurgery, stereostatic biopsy, irradiation, radiation therapy, reconstructive therapy, and the study of moving parts.

2) *Time-Varying 2-D Signals:* In video it is customary to model the time-varying 2-D signals as 3-D signals, to preserve spatial and temporal correlations.

3) *Robotics:* Robotics is one of the most rapidly growing areas of current technology. There is an increasing effort to use robots in more sophisticated applications. For such applications the availability of 3-D visual systems is necessary.

4) *Geophysics:* 3-D seismic data processing was shown to have many advantages over 2-D processing. 3-D migrated data describe more accurately the geology of the area under study, than corresponding 2-D data.

Therefore, it is important that 3-D signal processing techniques are developed. The design of efficient 3-D filters is starting to emerge. Hirano *et al.* [2] developed 3-D filters for TV-signal applications, based on cascade and/or parallel combinations of 1-D component filters. Pitas and Venetsanopoulos [3] introduced symmetries to the design of m-D filters, and designed good 3-D IIR spherically symmetric and fan filters, by optimization techniques.

Using various arrangements or transformations, a 1-D filter can be transformed into a higher dimensional filter. In Fig. 1, all possible transformations of a 1-D (analog or digital) filter to, at most a 3-D filter, are depicted. The objective is to obtain 3-D digital filters from 1-D prototypes.

To increase the dimensionality of a 1-D digital filter, various techniques can be used. One of them is based on a transformation of its coefficients, with respect to the additional dimensions. This technique has been used to design 2-D filters with predefined specifications from 1-D filters [4]. A second possible technique is to arrange, in parallel and/or in cascade, filters of low dimensionality, designed with respect to different dimensions. 3-D filters have been realized as parallel and/or cascade arrangements of 1-D filters, each one of which is designed with respect to one of the dimensions z_1, z_2, or z_3 [2].

Both of these techniques are employed, in this paper, to design 3-D filters with predefined specifications, using circularly symmetric filters designed on the basis of 2-D rotated filters. The first technique exploits coefficient transformations and yields spherically symmetric, fan, as well as other symmetric filters. The second uses cascade arrangements of 2-D rotated filters and yields only spherically symmetric filters. With respect to Fig. 1, both techniques can be considered as a transformation of a 1-D analog filter to 2-D analog filter, then to a 2-D digital filter (rotated filter) and, finally, a transition to a 3-D digital filter. The first design technique is presented in Sections I–VI. In Section I, some aspects of the 2-D rotated filters are presented. Sections II and III deal with the design of 3-D filters introducing the transformation functions applied to the coefficients of the 2-D rotated filter. The stability of the filter designed is studied in Section IV,

Manuscript received June 23, 1986; revised January 12, 1987. This work was supported by the Public Benefit Foundation, "Alexander S. Onassis."

The authors are with the Department of Electrical Engineering, University of Toronto, Toronto, Canada M5S 1A4.

IEEE Log Number 8717301.

0098-4094/87/1200-1452$01.00 ©1987 IEEE

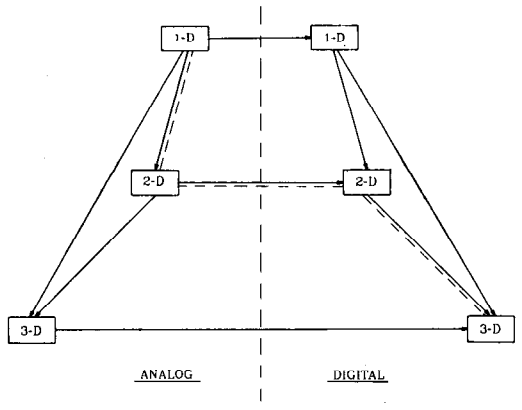

Fig. 1. Transformations increasing the dimensionality of a filter.

whereas the realization aspects are presented in Section V. Examples of spherically symmetric and fan filters designed on the basis of this technique are given in Section VI. Finally, Section VII deals with the second design technique based on cascade arrangements of 2-D rotated filters.

PART I—Design of 3-D Filters Using Coefficient Transformations of 2-D Rotated Filters

I. 1-D Cutoff Frequency and 2-D Band-Edge Contour

Any 1-D analog filter can be described by its transfer function, which is of the general form

$$H_1(s) = H_0 \frac{\prod_{i=1}^{m}(s - q_i)}{\prod_{j=1}^{n}(s - p_j)}. \tag{1.1}$$

For stability purposes, n must be greater than, or equal to m. The cutoff frequency of any 1-D analog filter depends only on the coefficients of the filter's transfer function. If the cutoff frequency of the analog filter is ω_c, then the transfer function (1.1), can be equivalently written as

$$H_1(s) = H_0\{\omega_c\} \frac{\prod_{i=1}^{m}(s - q_i\{\omega_c\})}{\prod_{j=1}^{n}(s - p_j\{\omega_c\})} \tag{1.2}$$

where the braces denote the dependence of the filter's coefficients on its cutoff frequency, and vice versa. Depending on the design technique, the relations of filter coefficients to cutoff frequency, can be analytically (Butterworth, Chebyshev) or numerically (computer-aided design) determined. By rotating clockwise the filter (1.2) and applying the bilinear transformation $s_i = (1 - z_i)/(1 + z_i)$ over each one of the resulting variables, the 2-D digital rotated filter can be obtained [5]. Its transfer function is of the form

$$H_2(z_1, z_2) = H_0\{\omega_c\} \prod_{i=1}^{n} \frac{a_0^i + a_1^i z_1 + a_2^i z_2 + a_{12}^i z_1 z_2}{b_0^i + b_1^i z_1 + b_2^i z_2 + b_{12}^i z_1 z_2} \tag{1.3}$$

where

$$n = \max\{m, n\}$$

$$\left.\begin{aligned} a_0^i &= \cos(\beta) - \sin(\beta) - q_i\{\omega_c\} \\ a_1^i &= \cos(\beta) + \sin(\beta) - q_i\{\omega_c\} \\ a_2^i &= -\cos(\beta) - \sin(\beta) - q_i\{\omega_c\} \\ a_{12}^i &= -\cos(\beta) + \sin(\beta) - q_i\{\omega_c\} \end{aligned}\right\}, \quad \text{for } 1 \leqslant i \leqslant m$$

$$a_0^i = a_1^i = a_2^i = a_{12}^i = 1, \quad \text{for } m < i \leqslant n$$

$$\left.\begin{aligned} b_0^i &= \cos(\beta) - \sin(\beta) - p_i\{\omega_c\} \\ b_1^i &= \cos(\beta) + \sin(\beta) - p_i\{\omega_c\} \\ b_2^i &= -\cos(\beta) - \sin(\beta) - p_i\{\omega_c\} \\ b_{12}^i &= -\cos(\beta) + \sin(\beta) - p_i\{\omega_c\} \end{aligned}\right\}, \quad \text{for } 1 \leqslant i \leqslant n.$$

Stable filters, rotated over any angle β, can be obtained (Appendix I1). Cascading a number of rotated filters based on the same 1-D elementary filter, whose rotation angles are distributed over 180°, results in a 2-D filter whose magnitude response approximates circular symmetry. The more rotated filters cascaded, the better the circular symmetry achieved. The transfer function of this filter is of the form

$$\hat{H}_2(z_1, z_2) = \prod_{l=1}^{L} H_2^l(z_1, z_2) \tag{1.4}$$

where $H_2^l(z_1, z_2)$ is given by (1.3). The only difference among the cascaded filters lies in their rotation angles β_i. In the Fourier transform domain of a 2-D filter, any contour on which

$$|H_2(\omega_1, \omega_2)| = \text{constant}$$

is called "isopotential contour." The specific filter designed is normalized ($\max|\hat{H}_2| = 1$). Its isopotential:

$$|\hat{H}_2(\omega_1, \omega_2)| = \frac{1}{\sqrt{2}}$$

which is called "band-edge contour" (corresponding to 1-D cutoff frequency), approximates a circle with radius ω_{c2D}. According to the design procedure, there is a monotonic relationship between ω_c and ω_{c2D}. The larger the value of ω_c, the larger the value of ω_{c2D}.

Let us define the function that relates ω_c to ω_{c2D} as

$$\omega_c = g(\omega_{c2D}). \tag{1.5}$$

This function can be numerically determined. For each value of the radius ω_{c2D} of the circle to be approximated by the band-edge contour of the filter designed, a value of the cutoff frequency ω_c of the elementary filter to be used is assigned. The proposed algorithm to compute ω_c is called Procedure I and comprises the following steps.

Procedure I

i) Read the value of ω_{c2D}.
ii) For the circularly symmetric filter under consideration, form the root mean square error (RMSE):

$$E = \frac{1}{2}\left[\sum_{i=1}^{2}\left(|\hat{H}_2(\omega_1, \omega_2)| - 0.707\right)^2\right]^{1/2} \tag{1.6}$$

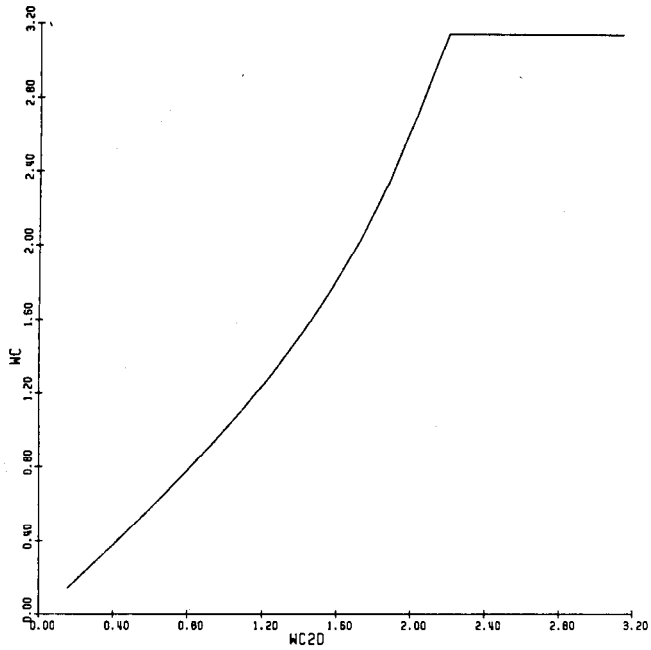

Fig. 2. Curve relating ω_{c2D} of a quadrantally symmetric filter to ω_c. Design based on the cascade of 2-D rotated filters.

at the points

$$(\omega_1, \omega_2) = \begin{cases} (\omega_{c2D}, 0) \\ \left(\frac{\omega_{c2D}}{\sqrt{2}}, \frac{\omega_{c2D}}{\sqrt{2}}\right). \end{cases} \tag{1.7}$$

iii) Minimize E with respect to ω_c.

The resulting ω_c, for a specific ω_{c2D}, is the value of the 1-D filter's cutoff frequency that must be used, so that the 2-D circularly symmetric filter designed (1.4) best approximates the circle with radius ω_{c2D}, by means of the RMSE.

In Fig. 2, the curve relating ω_{c2D} to ω_c for a circularly symmetric filter, is shown.

The 2-D filter is designed by cascading two rotated filters based on the same second-order Butterworth elementary filter; one rotated over $((3\pi/2)+(\pi/4))$ and the other over $((3\pi/2)-(\pi/4))$. This filter possesses quadrantal symmetry in is magnitude response [appendix II]. The 1-D elementary filter used, is not an ideal one. Furthermore, the bilinear transformation $s_i = (1-z_i)/(1+z_i)$ used to produce (1.3), slightly deforms the contour plots of the 2-D rotated filter. Keeping these imperfections in mind, one can easily realize that it is not possible to design a circularly symmetric filter, whose band-edge contour approximates a circle with radius very close to π. Hence, in Fig. 2, it is understood that there is not any value of ω_c, that results in a value of ω_{c2D} very close to π.

II. Design of 3-D Digital Filters

Suppose that we would like to design a 3-D filter, to meet the following specifications.

i) On any plane $\omega_3 = constant$, its magnitude response is circularly symmetric.

ii) Its band-edge contour, on any $\omega_3 = constant$, is a circle with radius:

$$\omega_{c2D} = f(\omega_3) \tag{2.1}$$

where $f(\omega_3)$ is periodic with period 2π.

Consider the 2-D circularly symmetric filter given by (1.4). This can be regarded as a 3-D filter independent of the third axis z_3. Its band-edge contour, for any $\omega_3 = constant$, approximates a circle with radius ω_{c2D}. The filter's coefficients depend on ω_{c2D}, since they depend on ω_c, which is a function of ω_{c2D} (1.5). To meet the above specifications, the radius ω_{c2D} must be related to ω_3 by means of (2.1). Change the coefficients of the rotated filter (1.3), so that, instead of constant ω_c, they are functions of

$$\omega_c = g(f(\omega_3)) \tag{2.2}$$

where $f(\cdot)$ and $g(\cdot)$ are functions given by (1.5) and (2.1), respectively. The resulting 3-D function, on the torus:

$$T^3 = \{(z_1, z_2, z_3); |z_1| = 1 \cap |z_2| = 1 \cap |z_3| = 1\}$$

is of the form

$$\hat{H}(\omega_1, \omega_2, \omega_3) = \prod_{l=1}^{L} H^l(\omega_1, \omega_2, \omega_3) \tag{2.3}$$

where $H^l(\omega_1, \omega_2, \omega_3)$ is the frequency response of a rotated filter given by (1.3), under the transformed coefficients:

$$\left.\begin{aligned} a_0^i(\omega_3) &= \cos(\beta) - \sin(\beta) - q_i[g(f(\omega_3))] \\ a_1^i(\omega_3) &= \cos(\beta) + \sin(\beta) - q_i[g(f(\omega_3))] \\ a_2^i(\omega_3) &= -\cos(\beta) - \sin(\beta) - q_i[g(f(\omega_3))] \\ a_{12}^i(\omega_3) &= -\cos(\beta) + \sin(\beta) - q_i[g(f(\omega_3))] \end{aligned}\right\},$$

for $1 \leqslant i \leqslant m$

$$a_0^i(\omega_3) = a_1^i(\omega_3) = a_2^i(\omega_3) = a_{12}^i(\omega_3) = 1,$$

for $m < i \leqslant n$

$$\left.\begin{aligned} b_0^i(\omega_3) &= \cos(\beta) - \sin(\beta) - p_i[g(f(\omega_3))] \\ b_1^i(\omega_3) &= \cos(\beta) + \sin(\beta) - p_i[g(f(\omega_3))] \\ b_2^i(\omega_3) &= -\cos(\beta) - \sin(\beta) - p_i[g(f(\omega_3))] \\ b_{12}^i(\omega_3) &= -\cos(\beta) + \sin(\beta) - p_i[g(f(\omega_3))] \end{aligned}\right\},$$

for $1 \leqslant i \leqslant n$.

The $\hat{H}(\omega_1, \omega_2, \omega_3)$ depends on all three dimensions and for any $\omega_3 = constant$, its band-edge contour approximates a circle with radius:

$$\omega_{c2D} = g^{-1}(\omega_c) = g^{-1}[g(f(\omega_3))] = f(\omega_3).$$

Consequently, this function meets all predefined specifications. In order that (2.3) represent the frequency response of a finite-extent 3-D digital filter, its coefficients must be expressed as finite-extent functions of $e^{(\pm j\omega_3)}$. There are two possible ways to achieve this representation. The first one is to approximate the coefficients (2.3b) by a 1-D rational function of ω_3 (IIR filter). The IIR filter used in this approximation must be both stable and inverse-stable (the $1/H(z_3)$ filter must be stable). The inverse stability requirement is posed in order to achieve, in later stages, a

stable 3-D filter. This point is better explained in Section I-D, that deals with the stability of the resulting 3-D filter. However, the inverse stability requirement might be relaxed, since, using 1-D cepsrum analysis, the 3-D filter obtained can be stabilized (see Section I-D). Since the implementation of this approach is in early stages, the results of this method are not presented in this paper.

The simplest possible way to express the coefficients (2.3b) as finite-extent functions of $e^{(\pm j\omega_3)}$ is by using windowed cosine Fourier series (FIR filter). For efficient approximations it is essential that:

i) the function $f(\omega_3)$ must be even, and
ii) the coefficients $[H_0\{\omega_c\}, q_i\{\omega_c\}$ and $p_i\{\omega_c\}]$ of the 1-D elementary filter must be simple functions of ω_c.

The first requirement constrains the magnitude responses that can be implemented, to be symmetric over the plane $\omega_3 = 0$. However, most of the responses to be approximated, such as spherically symmetric or fan responses, satisfy this requirement. To satisfy the second requirement, the poles and the zeros of the 1-D elementary filter used in the design, must not only depend on the filter's cutoff frequency, but also be simple functions of it. Hence, the most appropriate 1-D analog filter is the Butterworth filter. Its coefficients are of the form

$$\begin{aligned} H_0(\omega_c) &= \omega_c^n \\ q_i(\omega_c) &= 0 \\ p_i(\omega_c) &= C_i\omega_c \end{aligned} \tag{2.4}$$

where C_i is a complex number depending on the order n of the Butterworth filter. Furthermore, note that an increase of the order n, results in an increase of the number of coefficients (2.3b) which are approximated by windowed Fourier series, and, consequently, in a significant increase of the coefficients' number in the 3-D filter introduced. Therefore, in the proposed design technique, a second-order 1-D Butterworth is used as the elementary analog filter. However, the extension to any order Butterworth filter is straightforward.

For this particular choice,

$$\begin{aligned} n &= 2 \\ C_1 &= -\frac{\sqrt{2}}{2}(1-j) \\ C_2 &= -\frac{\sqrt{2}}{2}(1+j). \end{aligned} \tag{2.5}$$

For the coefficients (2.4), with $n = 2$, the following expansions into Fourier series, must be computed:

$$g(f(\omega_3)) \approx u(\omega_3) = \sum_{n=0}^{N} c_n \cos(n\omega_3) = \sum_{n=0}^{N} \frac{c_n}{2}[e^{jn\omega_3} + e^{-jn\omega_3}] \tag{2.6a}$$

$$g^2(f(\omega_3)) \approx v(\omega_3) = \sum_{m=0}^{M} d_m \cos(m\omega_3) = \sum_{m=0}^{M} \frac{d_m}{2}[e^{jm\omega_3} + e^{-jm\omega_3}] \tag{2.6b}$$

where, $u(\omega_3)$ and $v(\omega_3)$ represent the windowed Fourier series of $g(f(\omega_3))$ and $g^2(f(\omega_3))$, correspondingly. Alternatively, (2.6b) can be approximated by the first $M+1$ terms of the series

$$[g(f(\omega_3))]^2 \approx u^2(\omega_3) = \left[\sum_{n=0}^{N} \frac{c_n}{2}(e^{jn\omega_3} + e^{-jn\omega_3})\right]^2. \tag{2.6c}$$

Note that these functions are symmetric with respect to $\omega_3 = 0$, and periodic with period 2π.

The transfer function of the 3-D filter designed on the basis of a second-order Butterworth filter, is described by

$$\hat{H}(z_1, z_2, z_3) = \prod_{l=1}^{L} H^l(z_1, z_2, z_3) \tag{2.7}$$

where

$$\begin{aligned} H^l(z_1, z_2, z_3) &= H_0(z_3) \prod_{i=1}^{2} H_i^l(z_1, z_2, z_3) \\ &= H_0(z_3) \cdot \prod_{i=1}^{2} \frac{a_0^{il}(z_3) + a_1^{il}(z_3)z_1 + a_2^{il}(z_3)z_2 + a_{12}^{il}(z_3)z_1z_2}{b_0^{il}(z_3) + b_1^{il}(z_3)z_1 + b_2^{il}(z_3)z_2 + b_{12}^{il}(z_3)z_1z_2} \end{aligned} \tag{2.8a}$$

$$H_0(z_3) = \sum_{m=0}^{M} \frac{d_m}{2}(z_3^m + z_3^{-m}) \tag{2.8b}$$

$$\begin{aligned} a_0^{il}(z_3) &= 1 \\ a_1^{il}(z_3) &= 1 \\ a_2^{il}(z_3) &= 1 \\ a_{12}^{il}(z_3) &= 1 \\ b_0^{il}(z_3) &= \cos(\beta_l) - \sin(\beta_l) - C_i\left[\sum_{n=0}^{N} \frac{c_n}{2}(z_3^n + z_3^{-n})\right] \\ b_1^{il}(z_3) &= \cos(\beta_l) + \sin(\beta_l) - C_i\left[\sum_{n=0}^{N} \frac{c_n}{2}(z_3^n + z_3^{-n})\right] \\ b_2^{il}(z_3) &= -\cos(\beta_l) - \sin(\beta_l) - C_i\left[\sum_{n=0}^{N} \frac{c_n}{2}(z_3^n + z_3^{-n})\right] \\ b_{12}^{il}(z_3) &= -\cos(\beta_l) + \sin(\beta_l) - C_i\left[\sum_{n=0}^{N} \frac{c_n}{2}(z_3^n + z_3^{-n})\right]. \end{aligned} \tag{2.8c}$$

The design algorithm, based on the previous analysis, is called Procedure II and involves the following steps.

Procedure II

i) Design the 2-D circularly symmetric filter by rotating the same 1-D Butterworth filter over angles lying between 0 and π, and cascading the resulting rotated filters.
ii) Divide the ω_3 axis into N distinguished frequencies, uniformly distributed over $[0, \pi]$. N must be sufficiently large, to prevent space domain aliasing.

iii) For every distinct frequency ω_3^i, compute the corresponding ω_{c2D}^i from the function:

$$\omega_{c2D} = f(\omega_3).$$

iv) For every ω_{c2D}^i, using procedure I, compute numerically the corresponding cutoff frequency ω_c^i of the 1-D Butterworth filter, to be used on the plane $\omega_3 = \omega_3^i$.
At the end of this step, the sampled function $g(f(\omega_3^i))$, has been computed. The $g^2(f(\omega_3^i))$, can be then calculated easily.

v) To achieve the Fourier series decomposition (2.6), the inverse discrete Fourier transform (IDFT) can be employed. Since $f(\omega_3)$ is a periodic (with period 2π) and even function, the series $\{g(f(\omega_3^i))\}$ is periodic and symmetric. The DFT analysis and synthesis pairs of a periodic and symmetric discrete series x_n with period $2N-1$, are expressed as

$$X_k = x_0 + \sum_{n=1}^{N-1} 2x_n \cos\frac{2\pi kn}{2N-1}$$

with an IDFT given by

$$x_n = \frac{1}{2N-1}\left[X_0 + \sum_{k=1}^{N-1} 2X_k \cos\frac{2\pi kn}{2N-1}\right]$$

Using an IDFT routine for the series $\{X_k\} = \{g(f(\omega_3^k))\}$, the coefficients c_n of (2.6a) are computed. The coefficients d_m of (2.6b), are similarly calculated.

vi) Impose the series $\{c_n\}$ and $\{d_m\}$ on the coefficients of each rotated filter, as in (2.8), to obtain the transfer function of the 3-D filter that approximates the desired magnitude response.

III. Suboptimum Approach

Procedure II for the design of 3-D filters, is cumbersome. Steps iv) and v) require complicated numerical computations including nonlinear optimization and inverse DFT. Furthermore, if in some region of ω_3, $f(\omega_3)$ is close to π (as for example in the case of a 3-D fan filter), the magnitude response of the 3-D filter designed, does not exactly approximate the desired response. The reason for this inability is the implication of Fig. 2, that it is not possible to design circularly symmetric filters with ω_{c2D} very close to π, by cascading 2-D rotated filters. These imperfections encourage the development of a much less complicated, suboptimum procedure. In this approach, the relationship between the 1-D cutoff frequency ω_c and the 2-D band-edge radius ω_{c2D}, is assumed to be linear

$$\omega_{c2D} = \omega_c.$$

According to Fig. 2, this assumption is valid on a considerable frequency region. Hence, in (1.3) the transformation

$$\omega_c = f(\omega_3) \tag{3.1}$$

instead of (2.2), is applied. The Fourier series analysis of (3.1) can be now derived analytically, for simple functions $f(\omega_3)$, such as in the case of spherically symmetric or fan filters. The Fourier transform analysis pair is expressed by

$$f(\omega_3) = c_0 + \sum_{n=1}^{\infty} c_n \cos(n\omega_3) \tag{3.2a}$$

where

$$c_0 = \frac{1}{2\pi}\int_{-\pi}^{\pi} f(\omega_3)\, d\omega_3 \tag{3.2b}$$

and

$$c_n = \frac{1}{\pi}\int_{-\pi}^{\pi} f(\omega_3)\cos(n\omega_3)\, d\omega_3.$$

The series (3.2a) must be truncated (by windowing) to $N+1$ terms, i.e.,

$$f(\omega_3) = c_0 + \sum_{n=1}^{N} c_n \cos(n\omega_3). \tag{3.3}$$

The number N can be chosen so that the maximum approximation error:

$$E = \max\{f(\omega_3) - \hat{f}(\omega_3)\}, \qquad \text{in } 0 \leqslant \omega_3 \leqslant \pi \tag{3.4}$$

does not exceed an accuracy ϵ. Similar truncation must be carried out for the function $f^2(\omega_3)$. The new procedure, called Procedure III, involves the following steps.

Procedure III

i) Design the 2-D circularly symmetric filter by rotating the same 1-D Butterworth filter over angles lying between 0 and π, and cascading the resulting rotated filters.

ii) Compute (analytically) the series $\{c_n\}$ and $\{d_m\}$ from (3.2), for $f(\omega_3)$ and $f^2(\omega_3)$ correspondingly.

iii) Impose these series on the coefficients of each rotated filter, as in (2.8).

IV. Stability

The 3-D filter (2.7) is designed by cascading various filters $H^l(z_1, z_2, {}_3)$. Hence, $\hat{H}(z_1, z_2, z_3)$ is stable if and only if (iff) each one of the cascaded filters is stable. In general, $H^l(z_1, z_2, z_3)$ is a cascade of K pairs of conjugate 3-D filters with complex coefficients, and $I-2K$ 3-D filters with real coefficients.

$$H^l(z_1, z_2, z_3) = \prod_{i=1}^{K} H_i^l(z_1, z_2, z_3) H_i^{l*}(z_1^*, z_2^*, z_3^*) \cdot \prod_{j=1}^{I-2K} \mathrm{Re}\, H_j^l(z_1, z_2, z_3).$$

Therefore, $H^l(z_1, z_2, z_3)$ has real coefficients and it is sable iff each of $H_i^l(z_1, z_2, z_3)$ is stable. From (2.8a):

$$H_i^l(z_1, z_2, z_3) = \frac{a_0^{il}(z_3) + a_1^{il}(z_3)z_1 + a_2^{il}(z_3)z_2 + a_{12}^{il}(z_3)z_1z_2}{b_0^{il}(z_3) + b_1^{il}(z_3)z_1 + b_2^{il}(z_3)z_2 + b_{12}^{il}(z_3)z_1z_2}. \tag{4.1}$$

The filter's coefficients are given in (2.8c), with c_i defined in (2.6a). The function $u(\omega_3)$ is symmetric over its center

$\omega_3 = 0$, and $\mathrm{Re}\{C_i\} < 0$. The stability conditions of this filter, under causal implementation, are (Appendix I1):

$$u(\omega_3) > 0, \qquad \text{for } 0 \leqslant \omega_3 \leqslant \pi \tag{4.2a}$$

$$\frac{3\pi}{2} \leqslant \beta \leqslant 2\pi \tag{4.2b}$$

$$b_0^{il}(z_3) = \cos(\beta) - \sin(\beta) - C_i\left[\sum_{n=0}^{N} \frac{c_n}{2}(z_3^n + z_3^{-n})\right] \neq 0, \quad \text{in } |z_3| \leqslant 1. \tag{4.2c}$$

The approximation function $u(\omega_3)$ can be controlled so that (4.2a) is satisfied. The second condition is removed by applying data transformations [6]. The last condition is never satisfied, since $b_0^{il}(z_3)$ has zeros both inside and outside the unit circle $|z_3| = 1$. Hence, the filter designed is unstable. Furthermore, there is no direction of recursion [8] on which this filter can be stably realized. However, elaborating more on the nature of the image processing applications, a question arises whether or not BIBO stability is a fair requirement for filters used in this area. The signals (pictures) that image processing has to deal with, are of finite extent. Filtering such signals with even BIBO unstable filters does not result in an infinite-magnitude output. Hence, after filtering, a scaling factor can be applied, to restrain the output's magnitude within appropriate values. With these ideas in mind, it is understood that BIBO stability is a very restrictive requirement for systems to be used in image processing. In another contribution [13] the notion of practical-BIBO stability was introduced. According to this approach, the stability behavior of m-D systems having m-D inputs that are of unbounded duration in at most one variable, is considered. It was shown that practical-BIBO stability is less restrictive and more relevant for practical applications than the conventional one. Nevertheless, we proceed with the BIBO stabilization of the filter designed.

Stabilization Procedure:

The filter (4.1) can be stabilized by using an appropriate realization scheme for $b_0^{il}(z_3)$. The analysis is carried out in the case that an Ith order Butterworth filter is used in the design.

Each one of the cascaded filters $H^l(z_1, z_2, z_3)$ (2.8a), has real coefficients and can be represented by

$$H^l(z_1, z_2, z_3) = H^0(z_3) \prod_{i=1}^{I} \frac{A_i^l(z_1, z_2, z_3)}{B_i^l(z_1, z_2, z_3)} = H^0(z_3) \frac{A^l(z_1, z_2, z_3)}{B^l(z_1, z_2, z_3)} \tag{4.3}$$

where,

$$A^l(z_1, z_2, z_3) = \sum_{n=0}^{I} \sum_{m=0}^{I} \alpha_{n,m}^l z_1^n z_2^m \tag{4.4a}$$

$$B^l(z_1, z_2, z_3) = \sum_{n=0}^{I} \sum_{m=0}^{I} \beta_{n,m}^l(z_3) z_1^n z_2^m = \beta_{0,0}^l(z_3) + C^l(z_1, z_2, z_3). \tag{4.4b}$$

The stability conditions of this filter are (Appendix I1):

$$B^l(z_1, z_2, z_3) \neq 0, \qquad \text{for } |z_2| = |z_3| = 1 \cap |z_1| \leqslant 1 \tag{4.5a}$$

$$B^l(0, z_2, z_3) \neq 0, \qquad \text{for } |z_3| = 1 \cap |z_2| \leqslant 1 \tag{4.5b}$$

$$B^l(0, 0, z_3) \neq 0, \qquad \text{for } |z_3| \leqslant 1. \tag{4.5c}$$

If, for any $0 \leqslant \omega_3 \leqslant \pi$, the Fourier transform (2.6a) is strictly positive, i.e.,

$$u(\omega_3) > 0 \tag{4.6}$$

and the rotation angle β:

$$\frac{-3\pi}{4} \leqslant \beta \leqslant 2\pi \tag{4.7}$$

the first two stability conditions are satisfied[1] by (4.3), since they are satisfied by each one of $B_i^l(z_1, z_2, z_3)$ (Appendix I1). It is shown in Appendix I2, that the term $\beta_{0,0}^l(z_3)$, on the unit circle $|z_3| = 1$, can be analyzed into

$$\beta_{0,0}^l(z_3) = {}^1\beta^l(z_3)\,{}^1\beta^l(z_3^{-1}) \tag{4.8}$$

where ${}^1\beta^l(z_3)$ is recursively stable, i.e.,

$${}^1\beta^l(z_3) \neq 0, \qquad \text{in } |z_3| \leqslant 1. \tag{4.9}$$

Furthermore, ${}^1\beta^l(z_3^{-1})$ is recursively stable if it is implemented using a routine that recurses in the negative direction $(-n)$, with respect to the dimension z_3. Hence, $\beta_{0,0}^l$ is recursively stable, if it is realized as a cascade of the recursive filter $1/{}^1\beta^l(z_3)$ and the same filter recursing on the $(-n)$ direction. Alternatively, if the 3-D transformation $T(\cdot)$ is defined as

$$T\big(X(z_1, z_2, z_3)\big) = X(z_1, z_2, z_3^{-1}) \tag{4.10}$$

filtering on the $(-n)$ direction is equivalent to an input transformation, filtering on the $(+n)$ direction and an output transformation [6]. These operations are described by

$$\frac{1}{{}^1\beta^l(z_3^{-1})} = T\left[\frac{1}{{}^1\beta^l(z_3)} T\big(X(z_1, z_2, z_3)\big)\right]. \tag{4.11}$$

Since the transformation $T(\cdot)$ does not contribute into the magnitude response, it is clear that, under this realization,

$$\beta_{0,0}(z_3) \neq 0, \qquad \text{for } |z_3| \leqslant 1. \tag{4.12}$$

Hence, the stability condition (4.5c), is also satisfied.

Summarizing, the first two stability conditions are satisfied if (4.6) and (4.7) hold, whereas the third condition is satisfied if $\beta_{0,0}^l(z_3)$ is realized through (4.8), with ${}^1\beta^l(z_3)$ recursing in the positive and ${}^1\beta^l(z_3^{-1})$ recursing in the negative z_3 direction. The only way to achieve such a realization is by using iterative techniques. This realization scheme is analyzed in the following section.

[1] The conditions (4.5a) and (4.5b) are satisfied by means of marginal stability. If, due to coefficients' truncations, stability problems are detected, the nonessential singularities of the second kind are removed by slightly perturbing the coefficients (Appendix I1).

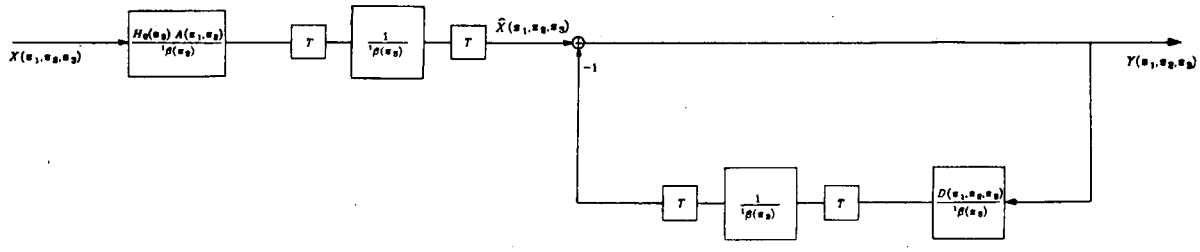

Fig. 3. Block diagram for stable realization of the 3-D filters designed.

V. Realization

Let $H(z_1, z_2, z_3)$ represent any of the cascaded filters $H^l(z_1, z_2, z_3)$ in (2.7). The conditions (4.6) and (4.7), are satisfied. This transfer function has real coefficients and can be written as

$$\begin{aligned} H(z_1, z_2, z_3) &= H_0(z_3)\frac{A(z_1, z_2)}{B(z_1, z_2, z_3)} \\ &= H_0(z_3)\frac{A(z_1, z_2)}{\beta(z_3)+D(z_1, z_2, z_3)} \\ &= \frac{H_0(z_3)A(z_1, z_2)}{\beta(z_3)}\frac{1}{1+\dfrac{D(z_1, z_2, z_3)}{\beta(z_3)}}. \end{aligned} \quad (5.1)$$

According to the previous section, $H(z_1, z_2, z_3)$ is stable, i.e.,

$$1+\frac{D(z_1, z_2, z_3)}{\beta(z_3)} \neq 0 \quad \text{in } \overline{U}^3$$

iff $1/\beta(z_3)$ is realized as

$$\frac{1}{\beta(z_3)} = \frac{1}{{}^1\beta(z_3)}\frac{1}{{}^1\beta(z_3^{-1})} = \frac{1}{{}^1\beta(z_3)}T\frac{1}{{}^1\beta(z_3)}T \quad (5.2)$$

where $T(\cdot)$ represents a data transformation on the direction z_3.

The block diagram representing this realization, is presented in Fig. 3.

The only part that needs further analysis is the feedback loop which is realized iteratively [7]. Define

$$F(z_1, z_2, z_3) = -\frac{D(z_1, z_2, z_3)}{{}^1\beta(z_3)}T\frac{1}{{}^1\beta(z_3)}T. \quad (5.3)$$

Since the data transformations do not contribute to the magnitude of $F(z_1, z_2, z_3)$, on $\overline{U}^3$,

$$|F(z_1, z_2, z_3)| = \left|\frac{D(z_1, z_2, z_3)}{[{}^1\beta(z_3)]^2}\right|. \quad (5.4)$$

The convergence of the iterative procedure that realizes the feedback loop, is now investigated. The analysis becomes much less cumbersome in the Fourier transform domain. The equation that governs the ith iteration is

$$\begin{aligned} Y^i(\omega_1, \omega_2, \omega_3) &= \hat{X}(\omega_1, \omega_2, \omega_3) \\ &\quad + F(\omega_1, \omega_2, \omega_3)Y_{i-1}(\omega_1, \omega_2, \omega_3) \end{aligned} \quad (5.5)$$

where $Y_i(\omega_1, \omega_2, \omega_3)$ and $\hat{X}(\omega_1, \omega_2, \omega_3)$ are the Fourier transforms of the output and the input of the loop, after the ith iteration, correspondingly. If initially $Y_0(\omega_1, \omega_2, \omega_3) = 0$, the output of the $(I+1)$th iteration will be

$$\begin{aligned} Y_{I+1}(\omega_1, \omega_2, \omega_3) &= \left[\sum_{i=0}^{I} F^{(I)}(\omega_1, \omega_2, \omega_3)\right]\hat{X}(\omega_1, \omega_2, \omega_3) \\ &= \frac{1-F^{(I+1)}(\omega_1, \omega_2, \omega_3)}{1-F(\omega_1, \omega_2, \omega_3)}\hat{X}(\omega_1, \omega_2, \omega_3). \end{aligned} \quad (5.6)$$

Therefore, the iterative procedure converges iff

$$|F(\omega_1, \omega_2, \omega_3)| < 1. \quad (5.7)$$

However, this is not a restrictive condition. Since, ${}^1\beta(z_3) \neq 0$ on the torus T^3, the function $|1-F(\omega_1, \omega_2, \omega_3)|$ has a maximum F_m:

$$F_m = \max\{|1-F(\omega_1, \omega_2, \omega_3)|\} < \infty. \quad (5.8)$$

The transfer function that describes the feedback loop is the following:

$$\begin{aligned} \tilde{H}(\omega_1, \omega_2, \omega_3) &= \frac{1}{1-F(\omega_1, \omega_2, \omega_3)} \\ &= \frac{1-F^*(\omega_1, \omega_2, \omega_3)}{[1-F(\omega_1, \omega_2, \omega_3)][1-F^*(\omega_1, \omega_2, \omega_3)]} \\ &= \frac{\lambda[1-F^*(\omega_1, \omega_2, \omega_3)]}{\lambda|1-F(\omega_1, \omega_2, \omega_3)|^2} \\ &= \frac{\lambda[1-F^*(\omega_1, \omega_2, \omega_3)]}{1-C(\omega_1, \omega_2, \omega_3)} \end{aligned} \quad (5.9)$$

where

$$0 < \lambda < \frac{2}{F_m^2}. \quad (5.10)$$

For the function $C(\omega_1, \omega_2, \omega_3)$ we derive

$$|C(\omega_1, \omega_2, \omega_3)| = |1-\lambda|1-F(\omega_1, \omega_2, \omega_3)|^2| < 1. \quad (5.11)$$

Hence, the iteration procedure described by (5.9), converges at

$$\begin{aligned} Y(\omega_1, \omega_2, \omega_3) &= \frac{\lambda[1-F^*(\omega_1, \omega_2, \omega_3)]}{1-C(\omega_1, \omega_2, \omega_3)}\hat{X}(\omega_1, \omega_2, \omega_3) \\ &= \frac{1}{1-F(\omega_1, \omega_2, \omega_3)}\hat{X}(\omega_1, \omega_2, \omega_3). \end{aligned} \quad (5.12)$$

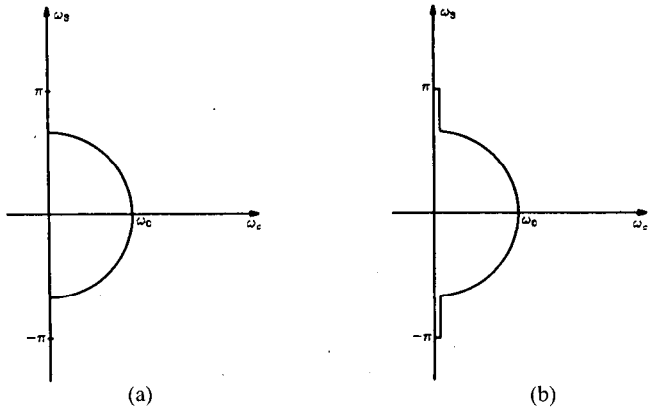

Fig. 4. Curve $\omega_c = f(\omega_3)$ in the case of sph. sym. filter design. (a) results in unstable, whereas (b) in stable realization.

Therefore, the feedback loop is realized using the converging iteration procedure.

VI. Examples

In this section we present examples of 3-D filter designed on the basis of the method proposed. A 1-D second-order Butterworth filter is used as the elementary filter. The circularly symmetric filter is designed as a cascade of two 2-D rotated filters, based on the same 1-D prototype; one rotated over 225° and the other over 315°. The second rotated filter is stable if it recurses in the $(+l, +n)$ direction (Appendix I1). The same filter can be used to achieve a rotation angle of 225° by rotating the input and the output arrays [6]. The frequency response of the cascade of these filters, is quadrantally symmetric (Appendix II). The quadrantally symmetric filter is transformed, by means of (3.1), as in Procedure 3.3, to obtain the 3-D filter. The Fourier series (3.2) and this corresponding to the function $f^2(\omega_3)$, are computed analytically.

Spherically Symmetric Filters

The function which gives the radius $\omega_{c2D}(\omega_3)$ of the circle, that the magnitude response of the filter designed approximates on any $\omega_3 = constant$ plane, is a periodic function, with period 2π. Furthermore, for $-\pi \leqslant \omega_3 \leqslant \pi$ it has the form of a semicircle with radius ω_0 (see Fig. 4(a)).

$$\omega_{c2D}(\omega_3) = f(\omega_3) = \begin{cases} \sqrt{\omega_0^2 - \omega_3^2}, & \text{for } |\omega_3| \leqslant \omega_0 \\ 0, & \text{for } |\omega_3| \geqslant \omega_0, \\ & \text{for } -\pi \leqslant \omega_3 \leqslant \pi. \end{cases} \tag{6.1}$$

This function is symmetric with respect to its center $\omega_3 = 0$, and can be analyzed into the Fourier series:

$$f(\omega_3) = \sum_{n=0}^{\infty} c_n \cos(n\omega_3). \tag{6.2}$$

The coefficients c_n, are computed as follows:

$$c_0 = \frac{1}{2\pi}\int_{-\pi}^{\pi} f(\omega_3)\, d\omega_3 = \frac{\omega_0^2}{4}. \tag{6.3}$$

and

$$c_n = \frac{1}{\pi}\int_{-\pi}^{\pi} f(\omega_3)\cos(n\omega_3)\, d\omega_3$$

$$= \frac{2}{\pi}\int_0^{\omega_0} \sqrt{\omega_0^2 - \omega_3^2}\cos(n\omega_3)\, d\omega_3.$$

Change the integration variable, using

$$\omega_3 = \omega_0 \sin\theta.$$

For the new integration variable:

$$c_n = \frac{2}{\pi}\int_0^{\pi/2} \omega_0^2 \cos(n\omega_0 \sin\theta)(\cos\theta)^2\, d\theta$$

$$= \frac{\omega_0^2}{\pi}\int_0^{\pi} \cos(n\omega_0 \sin\theta)(\cos\theta)^2\, d\theta. \tag{6.4}$$

It is well known that for $n > -\frac{1}{2}$

$$J_m(x) = \frac{x^m}{2^m\sqrt{\pi}\,\Gamma\left(m + \frac{1}{2}\right)}\int_0^{\pi} \cos(x\sin\theta)\cos^{2m}\theta\, d\theta$$

where $J_m(\cdot)$ is the Bessel function of first kind of order m and $\Gamma(\cdot)$ is the Gamma function.

With $m = 1$ and $\Gamma(1 + \frac{1}{2}) = \sqrt{\pi}/2$, (6.4) becomes

$$c_n = \frac{\omega_0}{n} J_1(n\omega_0). \tag{6.5}$$

If the filter designed is to be numerically implemented, the series (6.2) must be windowed to

$$u(\omega_3) = \sum_{n=0}^{N} c_n \cos(n\omega_3) \tag{6.6}$$

where c_n now represents the windowed coefficients of $f(\omega_3)$. For stability purposes,

$$u(\omega_3) > 0, \qquad \text{for } 0 \leqslant \omega_3 \leqslant \pi. \tag{6.7}$$

In the frequency transform domain, the windowing operation is described by

$$u(\omega_3) = \frac{1}{2\pi}\int_{-\pi}^{\pi} f(\theta) W(\omega_3 - \theta)\, d\theta \tag{6.8}$$

where $W(\omega_3)$ is the frequency response (spectrum) of the window applied on $f(\omega_3)$. Since

$$f(\omega_3) > 0, \qquad \text{for } -\pi \leqslant \omega_3 \leqslant \pi$$

a sufficient (not necessary) condition for the satisfaction of (6.7) is:

$$W(\omega_3) \geqslant 0, \qquad \text{for } -\pi \leqslant \omega_3 \leqslant \pi. \tag{6.9}$$

This is true for Bartlett (or triangular) window, but not true for other windows that provide better frequency response, such as Hamming, Hanning, or Kaiser.

In the specific case (6.1), the use of windows that do not satisfy (6.9), results in negative $u(\omega_3)$, for some ω_3. To provide the ability to use such windows, a small constant ϵ is added to $f(\omega_3)$ for $\omega_0 \leqslant \omega_3 \leqslant \pi$. Under this formulation, the functions $f(\omega_3)$ and $u(\omega_3)$ become

$$\hat{f}(\omega_3) = f(\omega_3) + \epsilon \tag{6.10}$$

$$\hat{u}(\omega_3) = \sum_{n=0}^{N} (c_n + d_n)\cos(n\omega_3) \tag{6.11}$$

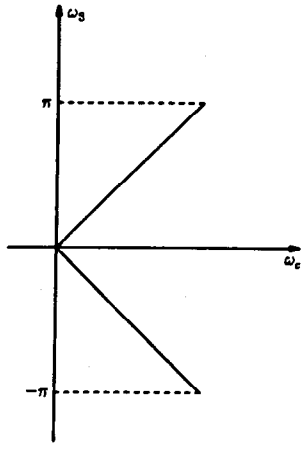

Fig. 5. Curve $\omega_c = f(\omega_3)$ in the case of 3-D fan filter design.

where

$$d_0 = \frac{\epsilon(\pi - \omega_0)}{\pi} \tag{6.12}$$

$$d_n = \frac{\cos(n\pi)\sin(n(\pi - \omega_0))}{n\pi}. \tag{6.13}$$

Finally, the spherically symmetric filter must be cascaded with a 1-D low-pass filter with cutoff frequency equal to ω_0, at the z_3 direction. This filter is used to eliminate the passband, around the ω_3 axis, introduced b the small number ϵ (see Fig. 4(b)).

The coefficients d_m of the Fourier series corresponding to $f^2(\omega_3)$, are similarly computed. Since $f^2(\omega_3)$ does not affect the stability, a simple rectangular window is used for its truncation. Hence,

$$v(\omega_3) = \sum_{m=0}^{M} d_m \cos(m\omega_3) \tag{6.14}$$

where

$$d_0 = \frac{1}{2\pi}\int_{-\pi}^{\pi}(\omega_0^2 - \omega_3^2)\, d\omega_3 = \frac{2}{3}\frac{\omega_0^3}{\pi} \tag{6.15}$$

and

$$d_m = \frac{1}{\pi}\int_{-\pi}^{\pi}(\omega_0^2 - \omega_3^2)\cos(m\omega_3)\, d\omega_3$$
$$= \frac{4}{\pi m^2}\left[-\omega_0\cos(m\omega_0) + \frac{1}{m}\sin(m\omega_0)\right]. \tag{6.16}$$

The first spherically symmetric filter, is one designed for $\omega_0 = 0.6\pi$. The small constant $\epsilon = 0.1E\text{-}2$ is added in the frequency response to be approximated, for $\omega_0 \leqslant \omega_3 \leqslant \pi$. A Kaiser window, of length $N = 20$, is used for the truncation of the series $\hat{f}(\omega_3)$. A Kaiser window is also used to obtain the truncated series $v(\omega_3)$. For this window, the value $M = 40$ is chosen. The cutoff frequency, of the 1-D low-pass filter, used to eliminate the passband around the ω_3 axis, introduced by ϵ, is equal to $(4/6)\omega_0$. The contour plots of the filter designed, on the planes $\omega_2 = 0$, $\omega_2 = \pi/4$ and $\omega_3 = 0$, are presented, respectively, in Fig. 6(a)–(c).

Fan Filters

The periodic function that relates ω_{c2D} to ω_3, in the case of fan filters, is shown in Fig. 5 and is described by

$$\omega_{c2D}(\omega_3) = f(\omega_3) = |\omega_3|, \qquad \text{for } -\pi \leqslant \omega_3 \leqslant \pi. \tag{6.17}$$

This is a symmetric over $\omega_3 = 0$ function, and can be written as

$$f(\omega_3) = \sum_{n=0}^{\infty} c_n \cos(n\omega_3). \tag{6.18}$$

The Fourier series analysis (3.2b), results in the coefficients:

$$c_0 = \frac{\pi}{2} \tag{6.19}$$

$$c_n = \frac{1}{\pi}\int_{-\pi}^{\pi}|\omega_3|\cos(n\omega_3)\, d\omega_3 = 2\frac{\cos(n\pi) - 1}{\pi n^2}. \tag{6.20}$$

To truncate this series, the windowing technique is used. The use of any kind of windows proved to result in a function $u(\omega_3)$, such that

$$u(\omega_3) = \sum_{n=0}^{N} c_n \cos(n\omega_3) > 0, \qquad \text{for } 0 \leqslant \omega_3 \leqslant \pi. \tag{6.21}$$

Similarly, the function $f^2(\omega_3)$ can be approximated by

$$f^2(\omega_3) \approx v(\omega_3) = \sum_{m=0}^{M} d_m \cos(m\omega_3) \tag{6.22}$$

where

$$d_0 = \frac{\pi^2}{3} \tag{6.23}$$

and

$$d_m = \frac{4}{m^2}\cos(m\pi). \tag{6.24}$$

The contour plots on the planes $\omega_2 = 0$ and $\omega_3 = 0.4\pi$, of a 90° fan filter, designed on the basis of the technique proposed, are presented in Fig. 7(a) and 7(b), correspondingly. Two rectangular windows, one of length $N = 20$, and the other of length $M = 40$, are used for the truncation of the series $f(\omega_3)$ and $f^2(\omega_3)$, in (6.21) and (6.22), respectively.

PART II—DESIGN OF 3-D SPHERICALLY SYMMETRIC FILTERS USING CASCADES OF 2-D CIRCULARLY SYMMETRIC FILTERS

VII. DESIGN OF 3-D FILTERS USING CASCADES

Consider the cascade $H_2(z_1, z_2)$ of two rotated filters, one rotated over an angle $\beta = 225°$ and the other over an angle $\beta + 90° = 315°$. This filter is designed with respect to the variables z_1 and z_2. Its magnitude response $F_2(\omega_1, \omega_2)$ is quadrantally symmetric (Appendix II) i.e.,

$$F_2(\omega_1, \omega_2) = F_2(-\omega_1, \omega_2) = F_2(\omega_1, -\omega_2) = F_2(\omega_2, \omega_1). \tag{7.1}$$

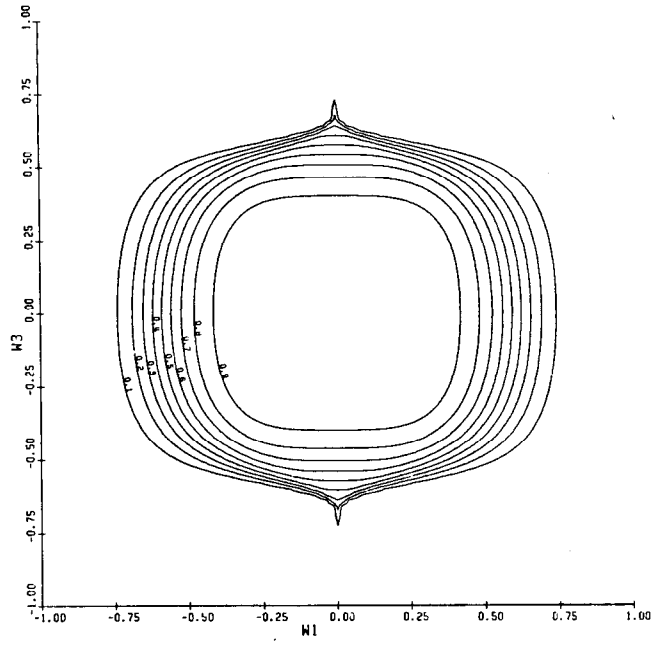

Fig. 6(a). Contour plots of 3-D spherically symmetric filter on $\omega_2 = 0$. Design based on prototype $\omega_0 = 0.6\pi$.

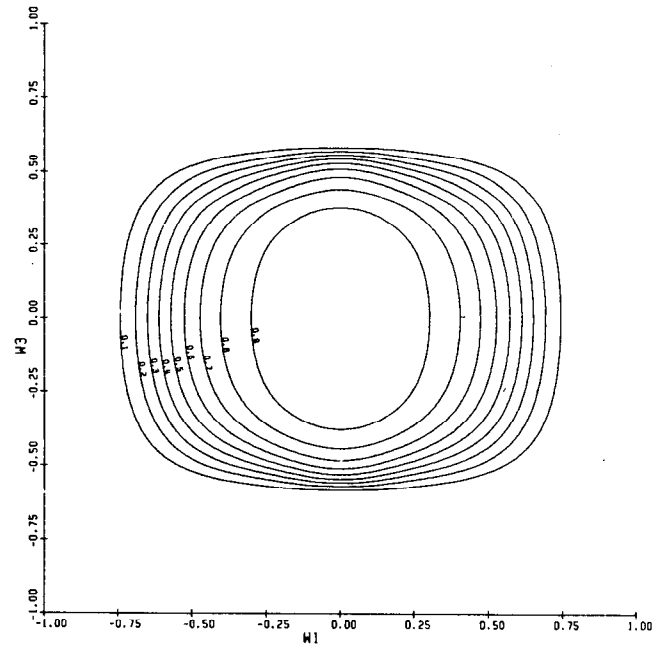

Fig. 6(b). Contour plots of 3-D spherically symmetric filter on $\omega_2 = \pi/4$. Design based on prototype $\omega_0 = 0.6\pi$.

Theorem 3.1: Consider the 2-D filter $H_2(z_1, z_2)$, whose magnitude response $F_2(\omega_1, \omega_2)$ is quadrantally symmetric. Form the 3-D digital filter as the cascade

$$H(z_1, z_2, z_3) = H_2(z_1, z_2)H_2(z_2, z_3)H_2(z_1, z_3). \quad (7.2)$$

Its 3-D magnitude response, given by

$$F_3(\omega_1, \omega_2, \omega_3) = F_2(\omega_1, \omega_2)F_2(\omega_2, \omega_3)F_2(\omega_3, \omega_1) \quad (7.3)$$

possesses 48-hedral symmetry.

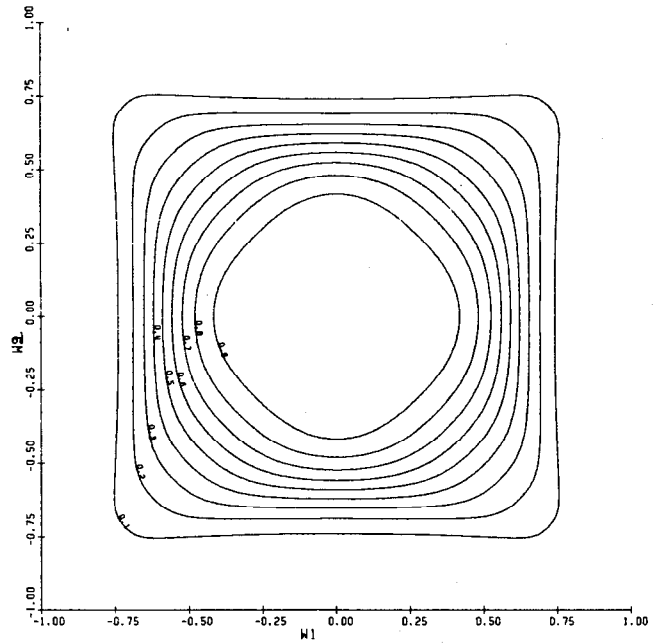

Fig. 6(c). Contour plots of 3-D spherically symmetric filter on $\omega_3 = 0$. Design based on prototype $\omega_0 = 0.6\pi$.

Proof: Combining (7.1) and (7.2), the following relations are easily derived:

$$\begin{aligned} &F_2(\omega_1, \omega_2)F_2(\omega_2, \omega_3)F_2(\omega_3, \omega_1) \\ &\quad = F_2(-\omega_1, \omega_2)F_2(\omega_2, \omega_3)F_2(\omega_3, -\omega_1) \\ &\quad = F_2(\omega_1, -\omega_2)F_2(-\omega_2, \omega_3)F_2(\omega_3, \omega_1) \\ &\quad = F_2(\omega_1, \omega_2)F_2(\omega_2, -\omega_3)F_2(-\omega_3, \omega_1) \\ &\quad = F_2(\omega_2, \omega_1)F_2(\omega_1, \omega_3)F_2(\omega_3, \omega_2) \\ &\quad = F_2(\omega_1, \omega_3)F_2(\omega_3, \omega_2)F_2(\omega_2, \omega_1) \end{aligned}$$

or equivalently,

$$F(\omega_1, \omega_2, \omega_3) = F(-\omega_1, \omega_2, \omega_3) = F(\omega_1, -\omega_2, \omega_3) = F(\omega_1, \omega_2, -\omega_3) = F(\omega_2, \omega_1, \omega_3) = F(\omega_1, \omega_3, \omega_2). \quad (7.4)$$

Note that any 2-D circularly symmetric filter can be used, to form the cascade (7.2). Furthermore, the better the circular symmetry of the 2-D filters cascaded in (7.2), the better the spherical symmetry of the 3-D filter designed.

The band-edge surface, i.e., the surface in the Fourier transform domain, on which

$$F(z_1, z_2, z_3) = \frac{1}{\sqrt{2}} \quad (7.5)$$

of the filter designed, approximates a sphere with radius ω_{c3D}. The value of ω_{c3D}, is monotonically dependent on the cutoff frequency ω_c, of the 1-D filter used in the design of the rotated filters. The curve that relates ω_{c3D} to ω_c, for the specific design procedure, is presented in Fig. 8.

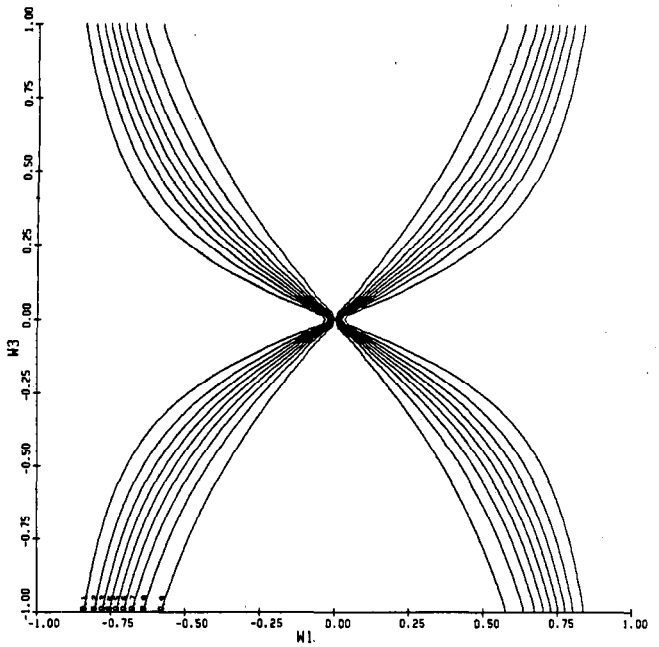

(a)

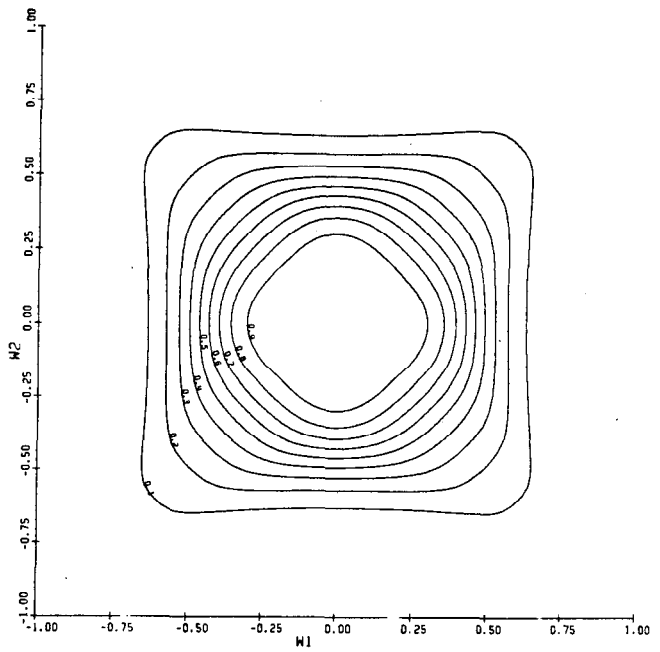

(b)

Fig. 7. (a) Contour plots of 3-D fan filter on $\omega_2 = 0$. (b) Contour plots of 3-D fan filter on $\omega_3 = 0.4\pi$.

For every (discrete) ω_{c3D}, the root mean square error:

$$E = \frac{1}{3}\left[\sum_{i=1}^{3}\left(F(\omega_1, \omega_2, \omega_3) - 0.707\right)^2\right]^{1/2} \tag{7.6}$$

is formed at the points:

$$(\omega_1, \omega_2, \omega_3) = \begin{cases} (\omega_{c3D}, 0, 0) \\ \left(\dfrac{\omega_{c3D}}{\sqrt{2}}, \dfrac{\omega_{c3D}}{\sqrt{2}}, 0\right) \\ \left(\dfrac{\omega_{c3D}}{\sqrt{3}}, \dfrac{\omega_{c3D}}{\sqrt{3}}, \dfrac{\omega_{c3D}}{\sqrt{3}}\right) \end{cases} \tag{7.7}$$

and minimized with respect to ω_c.

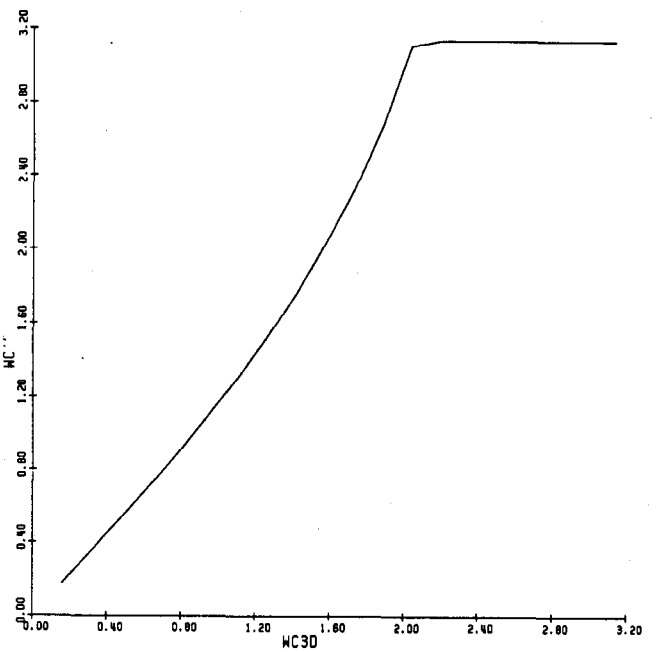

Fig. 8. Curve relating ω_{c3D} to ω_c.

On the basis of the technique proposed in this section, two spherically symmetric filters were designed. The first was designed using a 1-D Butterworth, with cutoff frequency $\omega_c = 0.6\pi$. Its contour plots, on the planes $\omega_3 = 0$ and $\omega_3 = \pi/2$, are presented in Fig. 9(a) and 9(b), respectively.

VIII. Conclusion

2-D recursive filters, possessing circular symmetry in their magnitude response, were designed by cascading 2-D rotated filters. Appropriate transformations of their coefficients, introducing the alternation of the filter's magnitude response with respect to the third variable, result in 3-D filters satisfying predefined specifications. Low-pass spherically symmetric and 3-D fan filters, are examples of filters that can be designed using the technique proposed. Each transformation function has the form of an 1-D FIR, zero-phase filter, whose frequency response approximates a specific function. These transformations introduce nonessential singularities of the second kind in the filter's transfer function. The BIBO stable implementation schemes proposed, were based on iterative procedures, and were derived using results of the 1-D cepstral analysis. Since the technique proposed can be used for the design of 3-D filters satisfying a wide range of specifications, an interesting topic under consideration is that of approximating the 1-D function by the magnitude response of an IIR filter. One possible way to achieve this representation is by using computer-aided design techniques. In this case, the filter designed as well as its inverse, must be BIBO stable.

On the basis of cascade arrangements of 2-D circularly symmetric filters, another technique was presented, for the

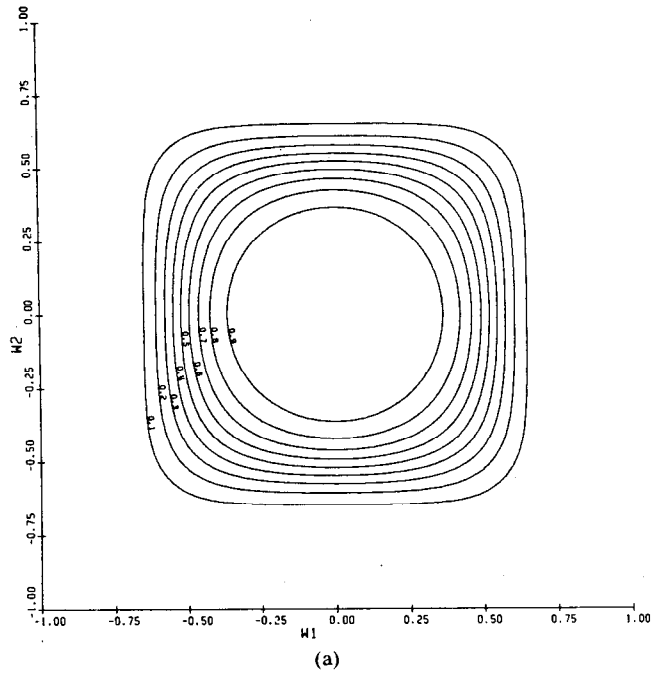

(a)

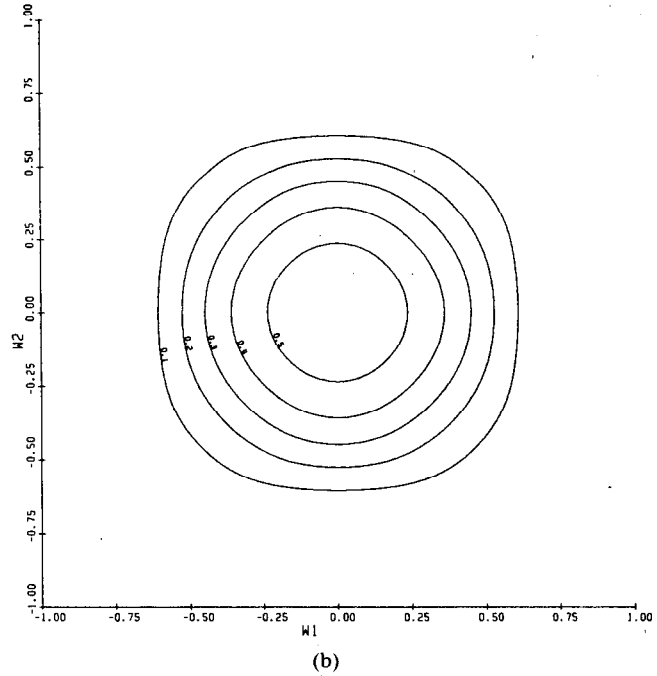

(b)

Fig. 9. (a) Contour plots of 3-D spherically symmetric filter on $\omega_3 = 0$. Design based on prototype $\omega_c = 0.6\pi$. (b) Contour plots of 3-D spherically symmetric filter on $\omega_3 = \pi/2$. Design based on prototype $\omega_c = 0.6\pi$.

design of 3-D spherically symmetric filters. Since the transfer function of the 3-D filter designed is separable, its stability is easily checked, by checking the stability of the 2-D filter. This design technique was illustrated by using circularly symmetric filters, designed on the basis of 2-D rotated filters.

At this point, it is interesting to make some comparisons among the filters designed using the various methods proposed. In Table I the number of filter coefficients, resulting in each technique under consideration, is presented.

TABLE I
COEFFICIENT COMPARISONS

FIR Without Symmetries	FIR With Symmetries	Transform. of 2-D Rotated Filters	Cascade of 2-D Rotated Filters	Cascade of 3-D Rotated Filters
$(2N+1)^3$	$(2N+1)^2$	$L(2M+1)+$ $4LI(2N+1)$	$24LI$	$8LI$

The first technique used for the design of 3-D FIR filters, is a modification of the McClellan transformation [1]. This transformation, readily extended to 3-D, results in filters with an enormous number of coefficients. The second technique utilizes the symmetries in the frequency response of the FIR filter to be designed, to significantly reduce both the design and the implementation costs [1]. The following two techniques are those introduced in this paper. The last design technique under comparison is based on cascade arrangements of 3-D rotated filters [12].

In the FIR case, the region of support of the 1-D filter used in the design is assumed $2N+1$. Note that the use of symmetries reduces the number of filter coefficients significantly. For the rest of the techniques that are based on rotated filters (2-D or 3-D), we assume that the 1-D IIR elementary filter used in the design, is of order I. Furthermore, we assume that the number of rotated filters cascaded is L. For the technique that transforms the coefficients of a circularly symmetric filter designed on the basis of 2-D rotated filters, the number of coefficients is computed from the cascade form (2.7) and (2.8). The numbers M and N refer to the regions of support of the finite-extent FIR filters used to approximate the functions of ω_3. In the next technique, the circularly symmetric filters are obtained by cascading L 2-D rotated filters, represented by (1.3). The number of filter coefficients in this case is computed from the cascade form (7.2). Finally, the last technique is based on cascade arrangements of L 3-D rotated filters.

From Table I we conclude that the methods using cascades of (2-D or 3-D) rotated filters result in 3-D filters with a small number of coefficients. However, these techniques can be used for the design of only spherically symmetric filters. The technique that exploits coefficient transformations of 2-D rotated filters can be used to approximate a wide range of specifications, yet resulting in filters with much smaller number of coefficients compared to the number of coefficients of a 3-D FIR filter. Since it is an analytic design technique, it does not possess the complexity of the computer aided design techniques that use numerical minimization methods to compute the filter's coefficients. This technique can be further simplified by using rational functions (transfer functions of 1-D IIR filters) to approximate the coefficients (2.3b) of the 2-D circularly symmetric rotated filter. The latest approach reduces significantly the number of 3-D filter's coefficients, so that it becomes a powerful design method in the sense of both reduced complexity of the resulting 3-D

filter, and capability to approximate a wide range of specifications.

Appendix I1

In this appendix, some stability aspects of 2-D rotated filters are reviewed, and the stability conditions for the 3-D rotated filters, are derived.

The rotated filter described by (1.3), with

$$\mathrm{Re}\{p_i\} < 0, \qquad \text{for } 1 \leqslant i \leqslant n \tag{I1.1}$$

is marginally stable (recursing in the $(+l, +m)$ direction), if and only if (iff)

$$270° \leqslant \beta \leqslant 360°. \tag{I1.2}$$

It is called marginally stable because it possesses a nonessential singularity of the second kind at the point $(z_1, z_2) = (-1, -1)$ [5]. However, this singularity does not pose any problems, since it can be easily removed by slightly perturbing the coefficients b_0^i and b_1^i [5]. Furthermore, [14] introduced transformations that result in rotated filters free from nonessential singularities of the second kind. Stable rotated filters, whose angle of rotation does not satisfy (I1.2), can be realized by using, either a routine that recurses in the appropriate direction, or an input and output data transformation [6].

Theorem I1.1

Let $H(z_1, z_2, z_3)$ be a 3-D filter of the form

$$H(z_1, z_2, z_3) = \frac{A(z_1, z_2, z_3)}{B(z_1, z_2, z_3)} = \frac{a_0(z_3) + a_1(z_3)z_1 + a_2(z_3)z_2 + a_{12}(z_3)z_1, z_2}{b_0(z_3) + b_1(z_3)z_1 + b_2(z_3)z_2 + b_{12}(z_3)z_1, z_2} \tag{I1.3}$$

where $a_i(z_3)$ are complex coefficients and $b_i(z_3)$ are of the form

$$b_0(z_3) = \cos(\beta) - \sin(\beta) - C_i\left[\sum_{n=0}^{N} \frac{c_n}{2}(z_3^n + z_3^{-n})\right] \tag{I1.4a}$$

$$b_1(z_3) = \cos(\beta) + \sin(\beta) - C_i\left[\sum_{n=0}^{N} \frac{c_n}{2}(z_3^n + z_3^{-n})\right] \tag{I1.4b}$$

$$b_2(z_3) = -\cos(\beta) - \sin(\beta) - C_i\left[\sum_{n=0}^{N} \frac{c_n}{2}(z_3^n + z_3^{-n})\right] \tag{I1.4c}$$

$$b_{12}(z_3) = -\cos(\beta) + \sin(\beta) - C_i\left[\sum_{n=0}^{N} \frac{c_n}{2}(z_3^n + z_3^{-n})\right]. \tag{I1.4d}$$

With

$$\mathrm{Re}\{C_i\} < 0 \tag{I1.5a}$$

and

$$\sum_{n=0}^{N} \frac{c_n}{2}(e^{jn\omega_3} + e^{-jn\omega_3}) = u(\omega_3) \tag{I1.5b}$$

the filter $H(z_1, z_2, z_3)$ is marginally stable, iff

$$u(\omega_3) > 0, \qquad \text{for } 0 \leqslant \omega_3 \leqslant \pi \tag{I1.6a}$$

$$270° \leqslant \beta \leqslant 360° \tag{I1.6b}$$

$$b_0(z_3) = \cos(\beta) - \sin(\beta) - C_i\left[\sum_{n=0}^{N} \frac{c_n}{2}(z_3^n + z_3^{-n})\right] \neq 0, \quad \text{in } |z_3| \leqslant 1. \tag{I1.6c}$$

Furthermore, this filter is unstable.

Proof:

The filter (I1.3) is associated with the causal filter [8]:

$$H(z_1, z_2, z_3) = \frac{\sum_{n_1=0}^{1}\sum_{n_2=0}^{1}\sum_{n_3=-N}^{N} a_{n_1,n_2,n_3} z_1^{n_1} z_2^{n_2} z_3^{n_3}}{\sum_{m_1=0}^{1}\sum_{m_2=0}^{1}\sum_{m_3=-M}^{M} b_{m_1,m_2,m_3} z_1^{m_1} z_2^{m_2} z_3^{m_3}} \tag{I1.7}$$

$$= \frac{z_3^{-N}\sum_{n_1=0}^{1}\sum_{n_2=0}^{1}\sum_{n_3=0}^{2N} a_{n_1,n_2,n_3-N} z_1^{n_1} z_2^{n_2} z_3^{n_3}}{z_3^{-M}\sum_{m_1=0}^{1}\sum_{m_2=0}^{1}\sum_{m_3=0}^{2M} b_{m_1,m_2,m_3-M} z_1^{m_1} z_2^{m_2} z_3^{m_3}}$$

$$= z_3^{M-N}\tilde{H}(z_1, z_2, z_3). \tag{I1.8}$$

The poles and the zeros of $H(z_1, z_2, z_3)$ and $\tilde{H}(z_1, z_2, z_3)$ are identical. Thus if $H(z_1, z_2, z_3)$ is implemented as causal filter, its stability conditions are given by [9]

$$B(z_1, z_2, z_3) \neq 0, \qquad \text{for } |z_2| = |z_3| = 1 \cap |z_1| \leqslant 1 \tag{I.9a}$$

$$B(0, z_2, z_3) \neq 0, \qquad \text{for } |z_3| = 1 \cap |z_2| \leqslant 1 \tag{I1.9b}$$

$$B(0, 0, z_3) \neq 0, \qquad \text{for } |z_3| \leqslant 1. \tag{I1.9c}$$

The first two conditions are tested for $|z_3| = 1$. For any ω_3, the coefficients of $H(z_1, z_2, e^{-j\omega_3})$ are identical to those of the 2-D rotated filter (1.3), with

$$p_i = C_i u(\omega_3). \tag{I1.10}$$

Therefore, the first two stability conditions, for any ω_3, are identical to those of a 2-D rotated filter, which are satisfied iff (I1.1) and (I1.2) hold. Consequently, (I1.9a) and

(I1.9b) are satisfied[2] if and only if:

$$u(\omega_3) > 0, \qquad \text{for } 0 \leqslant \omega_3 \leqslant \pi \tag{I1.11a}$$

and

$$270° \leqslant \beta \leqslant 360°. \tag{I1.11b}$$

Furthermore, the third stability condition requires that

$$B(0,0,z_3) = b_0(z_3) = \cos(\beta) - \sin(\beta) - C_i\left[\sum_{n=0}^{N} \frac{c_n}{2}(z_3^n + z_3^{-n})\right] \neq 0, \qquad \text{for } |z_3| \leqslant 1. \tag{I1.11c}$$

Hence, the stability conditions of $H(z_1, z_2, z_3)$ are those in (I1.3).

However, if z_3^0 is a zero of $b_0(z_3)$, then its inverse $\{z_3^0\}^{-1}$ is a zero of $b_0(z_3)$ too. Hence, (I1.11c) is never satisfied. The filter $H(z_1, z_2, z_3)$ in (I1.3), is unstable.

Appendix I2

In this appendix, some results from the cepstrum analysis of a stable function are reviewed and a stabilization procedure for the 3-D filters designed in Section III, is developed.

1-D Cepstrum Analysis

The cepstrum analysis has been carried out for both 1-D and 2-D cases [10], [11].

Suppose a function, ${}^1b = \{{}^1b_n\}_{n \geqslant 0}$, periodically sampled on the positive direction, where

$$\sum_{n=0}^{\infty} |{}^1b_n| < \infty. \tag{I2.1}$$

Its z-transform

$${}^1\beta(z) = \sum_{n=0}^{\infty} {}^1b_n z^n \tag{I2.2}$$

is called recursively stable if

$$|{}^1\beta(z)| \neq 0, \qquad \text{for } |z| \leqslant 1. \tag{I2.3}$$

In this case, the filter

$$H(z) = \frac{1}{{}^1\beta(z)}$$

is BIBO stable.

The 1-D cepstrum of ${}^1\beta(z)$ is defined by

$${}^1\hat{\beta}(z) = \ln\{{}^1\beta(z)\}. \tag{I2.4}$$

[2] Recall that these conditions are not completely satisfied. However, the nonessential singularities of the second kind can be easily removed.

According to this definition, the product in z-domain is equivalent ($\Rightarrow$) to addition in the cepstrum-domain:

$${}^1\beta(z) = {}^1\beta_1(z)\,{}^1\beta_2(z) \Rightarrow {}^1\hat{\beta}(z) = {}^1\hat{\beta}_1(z) + {}^1\hat{\beta}_2(z). \tag{I2.5}$$

Theorem I2.1 [10]

The power series ${}^1\beta(z)$ in (I2.2) is recursively stable iff there exists a power series

$${}^1\hat{\beta}(z) = \sum_{n=0}^{\infty} {}^1\hat{b}_n z^n \tag{I2.6}$$

that is absolutely convergent and equal to $\ln\{{}^1\beta(z)\}$ for $|z| \leqslant 1$.

Suppose now a function, ${}^2b = \{{}^2b_n\}_{n \leqslant 0}$, periodically sampled on the negative direction, and absolutely convergent. Its z-transform is of the form

$${}^2\beta(z^{-1}) = \sum_{n=0}^{\infty} {}^2b_{-n} z^{-n}. \tag{I2.7}$$

Corollary I2.1 [10]

The power series ${}^2\beta(z^{-1})$ is recursively stable (recursing in the negative direction) iff ${}^2\beta(z)$ is recursively stable, i.e., there exists a power series of the form

$${}^2\hat{\beta}(z) = \sum_{n=0}^{\infty} {}^2\hat{b}_n z^n \tag{I2.8}$$

that is absolutely convergent and equal to $\ln\{{}^2\beta(z)\}$ for $|z| \leqslant 1$. Consequently, the series

$${}^2\hat{\beta}(z^{-1}) = \sum_{n=0}^{\infty} {}^2\hat{b}_n z^{-n}$$

is absolutely convergent and equal to $\ln\{{}^2\beta(z^{-1})\}$ for $|z| \geqslant 1$.

Corollary I2.2 [10]

Suppose that the absolutely convergent power series is given, such that:

$$\sum_{n=0}^{\infty} {}^1\hat{b}_n z^n = \ln\{{}^1\beta(z)\} \qquad \text{for } |z| \leqslant 1. \tag{I2.9}$$

Form the series $\{{}^1b_n\}_{n \geqslant 0}$ as

$${}^1b_0 = \exp({}^1\hat{b}_0) \tag{I2.10a}$$

$${}^1b_p = \sum_{m=1}^{p} (m/p)\,{}^1\hat{b}_m\,{}^1b_{p-m}, \qquad p \neq 0 \tag{I2.10b}$$

This series is absolutely convergent and converges to

$$\sum_{n=0}^{\infty} {}^1b_n z^n = {}^1\beta(z), \qquad \text{for } |z| \leqslant 1. \tag{I2.11}$$

Suppose, on the other side, the absolutely convergent power series $\{{}^2\hat{b}_{-n}\}_{n=0}^{\infty}$ that converges to

$$\sum_{n=0}^{\infty} {}^2\hat{b}_{-n} z^{-n} = \ln\{{}^2\beta(z^{-1})\}, \qquad \text{for } |z| \geqslant 1 \tag{I2.12a}$$

where ${}^2\beta(z^{-1})$ is the z-transform of a function, periodically sampled on the negative direction, as in (I2.7). Then, the transformation by means of (I2.10) (with negative p and m), results in the absolutely convergent series

$\{{}^2b_{-n}\}_{n=0}^{\infty}$, that converges to

$$\sum_{n=0}^{\infty} {}^2b_{-n}z^{-n} = {}^2\beta(z^{-1}), \qquad \text{for } |z| \geq 1. \quad \text{(I2.12b)}$$

This is readily proved, since (I2.12a) can be equivalently written as

$$\sum_{n=0}^{\infty} {}^2\hat{b}_{-n}z^{n} = \ln\{{}^2\beta(z)\}, \qquad \text{for } |z| \leq 1$$

which is identical to (I2.9).

Stabilization Procedure

The procedure is carried out for the general case, that an Ith-order Butterworth filter is used in the design.

Each transformed rotated filter is described by a transfer function similar to (2.8a)

$$H^l(z_1, z_2, z_3) = H_0(z_3)\prod_{i=1}^{I} H_i^l(z_1, z_2, z_3) = H_0(z_3) \cdot \prod_{i=1}^{I} \frac{a_0^{il}(z_3) + a_1^{il}(z_3)z_1 + a_2^{il}(z_3)z_2 + a_{12}^{il}(z_3)z_1z_2}{b_0^{il}(z_3) + b_1^{il}(z_3)z_1 + b_2^{il}(z_3)z_2 + b_{12}^{il}(z_3)z_1z_2}. \quad \text{(I2.13)}$$

Each filter's coefficients are given by (2.8c). Since a Butterworth elementary filter is used in the design, C_i belongs to the set:

$$\{C_i\} = \{C_i; C_i^{(2I)} + 1 = 0 \cap \mathrm{Re}[C_i] < 0\}. \quad \text{(I2.14)}$$

Each one of the angles β_l lies between $3\pi/2$ and 2π. Furthermore, the Fourier transform:

$$u(\omega_3) = \sum_{n=0}^{N} \frac{c_n}{2}(e^{jn\omega_3} + e^{-jn\omega_3}) > 0 \quad \text{(I2.15)}$$

is provided. Each one of the filters $H^l(z_1, z_2, z_3)$ can be brought to the form

$$H(z_1, z_2, z_3) = H_0(z_3)\frac{A(z_1, z_2, z_3)}{B(z_1, z_2, z_3)} \quad \text{(I2.16)}$$

where $H_0(z_3)$ is given by (2.8b) and

$$A(z_1, z_2) = \sum_{n=0}^{I}\sum_{m=0}^{I} \alpha_{n,m}z_1^n z_2^m \quad \text{(I2.17a)}$$

$$B(z_1, z_2, z_3) = \sum_{n=0}^{I}\sum_{m=0}^{I} \beta_{n,m}(z_3)z_1^n z_2^m. \quad \text{(I2.17b)}$$

Theorem I2.2

The coefficient $\beta_{0,0}(z_3)$ of $B(z_1, z_2, z_3)$, on the unit circle $|z_3| = 1$, can be analyzed into the product $\tilde{\beta}_{0,0}(z_3)$ of two functions ${}^1\beta(z_3)$ and ${}^1\beta(z_3^{-1})$, where

$${}^1\beta(z_3) \neq 0, \qquad \text{in } |z_3| \leq 1. \quad \text{(I2.18)}$$

If $\beta_{0,0}(z_3)$ is substituted by $\tilde{\beta}_{0,0}(z_3)$, and $H(z_1, z_2, z_3)$ is implemented in a way that ${}^1\beta(z_3)$ is recursing in the positive, whereas ${}^2\beta(z_3^{-1})$, is recursing in the negative direction with respect to z_3, then $H(z_1, z_2, z_3)$ is (marginally)[3] stable, i.e.,

$$B(z_1, z_2, z_3) \neq 0, \qquad \text{in } \cap|z_i| \leq 1. \quad \text{(I2.19)}$$

Proof:

The stability conditions of $H(z_1, z_2, z_3)$ expressed by (I2.16) are (appendix I1):

$$B(z_1, z_2, z_3) \neq 0, \qquad \text{for } |z_2| = |z_3| = 1 \cap |z_1| \leq 1 \quad \text{(I2.20a)}$$

$$B(0, z_2, z_3) \neq 0, \qquad |z_3| = 1 \cap |z_2| \leq 1 \quad \text{(I2.20b)}$$

$$B(0, 0, z_3) \neq 0, \qquad \text{for } |z_3| \leq 1. \quad \text{(I2.20c)}$$

The first two conditions are satisfied by $B(z_1, z_2, z_3)$ (by means of marginal stability), since they are satisfied by each one of the cascaded denominators $B_i(z_1, z_2, z_3)$ (appendix I1).

The third stability condition requires that $\beta_{0,0}(z_3)$ be recursively stable, i.e.,

$$\beta_{0,0}(z_3) = \prod_{i=1}^{I} b_0^i(z_3) \neq 0, \qquad \text{for } |z_3| \leq 1. \quad \text{(I2.21)}$$

Let $H_i(z_1, z_2, z_3)$ be a complex-coefficients transfer function, a factor of the product (I2.13). The transfer function $H_i^*(z_1^*, z_2^*, z_3^*)$, where $(*)$ denotes complex conjugate, is also a factor of the same product. Hence, the coefficients of $H(z_1, z_2, z_3)$ in (I2.13) are real.

The specific coefficient $\beta_{0,0}(z_3)$, is given by

$$\beta_{0,0}(z_3) = \prod_{i=1}^{I} b_0^i = \prod_{i=1}^{I} \cos(\beta) - \sin(\beta) - C_i\left[\sum_{n=0}^{N} \frac{c_n}{2}(z_3^n + z_3^{-n})\right] = \sum_{n=-NI}^{NI} b_n z_3^n. \quad \text{(I2.22)}$$

Note that $b_n = b_{-n}$. Consequently,

$$\beta_{0,0}(z_3) = \beta_{0,0}(z_3^{-1}). \quad \text{(I2.23)}$$

On the unit circle $|z_3| = 1$,

$$\beta_{0,0}(\omega_3) = \prod_{i=1}^{I} \cos(\beta) - \sin(\beta) - C_i u(\omega_3). \quad \text{(I2.24)}$$

If C_i is complex, then both factors, one corresponding to C_i and the other to C_i^*, are included in the product (I2.24). The product of these two factors is a real number, equal to the squared magnitude of each one of them.

$$b_0^i(\omega_3)[b_0^i(\omega_3)]^* = (\cos(\beta) - \sin(\beta))^2 + [|C_i|u(\omega_3)]^2 > 0.$$

If C_i is real, then it is negative. Consequently, the factor corresponding to C_i:

$$b_0^i(\omega_3) = \cos(\beta_l) - \sin(\beta_l) - C_i u(\omega_3) > 0$$

since for $3\pi/2 \leq \beta \leq 2\pi$, $\cos(\beta) - \sin(\beta) > 0$. Therefore,

[3] The nonessential singularities of the second kind that may cause unstability, are easily removed through a small perturbation of the filter's coefficients (Appendix I1).

on the unit circle $|z_3|=1$, $\beta_{0,0}(z_3)$ is zero phase, strictly positive number.

$$\beta_{0,0}(\omega_3) > 0. \tag{I2.25}$$

The cepstrum $\hat{\beta}_{0,0}(z_3)$ of $\beta_{0,0}(z_3)$ is readily obtained, by evaluating its z-transform on the unit circle $|z_3|=1$.

$$\hat{\beta}_{0,0}(\omega_3) = \ln[\beta_{0,0}(\omega_3)] = \ln\left[\sum_{n=-2N}^{2N} b_n e^{-jn\omega_3}\right]. \tag{I2.26}$$

From (I2.23) and (I2.26), it is easily verified that

$$\hat{\beta}_{0,0}(\omega_3) = \hat{\beta}_{0,0}(-\omega_3). \tag{I2.27}$$

The logarithm does not present any problem, since $\beta_{0,0}(\omega_3)$ is real and strictly positive. Since $\beta_{0,0}(\omega_3) \neq 0$, all derivatives of $\hat{\beta}_{0,0}(\omega_3)$ are continuous. Hence, the following analysis into a Fourier series can be carried out:

$$\hat{\beta}_{0,0}(\omega_3) = \sum_{n=-\infty}^{\infty} \hat{b}_n e^{-jn\omega_3} \tag{I2.28}$$

where

$$\hat{b}_n = \frac{1}{2\pi}\int_{-\pi}^{\pi} \hat{\beta}_{0,0}(\omega_3) e^{jn\omega_3}\, d\omega_3. \tag{I2.29}$$

From (I2.27) and (I2.29) it is verified that

$$\hat{b}_n = \hat{b}_{-n}. \tag{I2.30}$$

Lemma

The series $\{\hat{b}_n\}_{n=0}^{\infty} = \{\hat{b}_{-n}\}_{n=0}^{\infty}$ is absolutely convergent.

Proof:

The function $\hat{\beta}_{0,0}(\omega_3)$ has continuous derivatives.

$$|\hat{b}_0| = \frac{1}{\pi}\left[\int_0^{\pi} \hat{\beta}_{0,0}(\omega_3)\, d\omega_3\right] = G_1.$$

In general,

$$\begin{aligned}
|\hat{b}_n| &= \frac{1}{\pi}\left|\int_0^{\pi} \hat{\beta}_{0,0}(\omega_3)\cos(n\omega_3)\, d\omega_3\right| \\
&= \frac{1}{n\pi}\left|\int_0^{\pi} \hat{\beta}_{0,0}(\omega_3)\, d\sin(n\omega_3)\right| \\
&= \frac{1}{n\pi}\left|\int_0^{\pi} \hat{\beta}'_{0,0}(\omega_3)\sin(\omega_3)\, d\omega_3\right| \\
&= \frac{1}{n^2\pi}\left|\int_0^{\pi} \hat{\beta}'_{0,0}(\omega_3)\, d\cos(n\omega_3)\right| \\
&= \frac{1}{n^2\pi}\left|\{\hat{\beta}'_{0,0}(\omega_3)\cos(n\omega_3)\}_0^{\pi}\right. \\
&\quad \left. - \int_0^{\pi} \hat{\beta}''_{0,0}(\omega_3)\cos(n\omega_3)\, d\omega_3\right| \\
&\leq \frac{1}{n^2\pi}\left[\left|\hat{\beta}'_{0,0}(\pi)\cos(n\pi) - \hat{\beta}'_{0,0}(0)\right|\right. \\
&\quad \left. + \left|\int_0^{\pi} \hat{\beta}''_{0,0}(\omega_3)\cos(n\omega_3)\, d\omega_3\right|\right] \\
&\leq \frac{1}{n^2\pi}\left[B + \left|\int_0^{\pi} \hat{\beta}''_{0,0}(\omega_3)\cos(n\omega_3)\, d\omega_3\right|\right] \\
&\leq \frac{1}{n^2\pi}\left[B + \int_0^{\pi} |\hat{\beta}''_{0,0}(\omega_3)|\, d\omega_3\right] = \frac{G_2}{n^2}.
\end{aligned}$$

Summarizing, if $M = \max(G_1, G_2)$,

$$|\hat{b}_0| \leq M$$

$$|\hat{b}_n| \leq \frac{M}{n^2}.$$

Hence, the series $\{\hat{b}_n\}_{n=0}^{\infty}$ is absolutely convergent, i.e.,

$$\sum_{n=0}^{\infty} |\hat{b}_n| < \infty. \tag{I2.31}$$

Consequently, the decomposition,

$$\begin{aligned}
\hat{\beta}_{0,0}(z_3) &= \frac{1}{2}\hat{b}_0 + \sum_{n=1}^{\infty} \hat{b}_n z_3^n + \frac{1}{2}\hat{b}_0 + \sum_{n=1}^{-\infty} \hat{b}_n z_3^n \\
&= \sum_{n=0}^{\infty} {}^1\hat{b}_n z_3^n + \sum_{n=0}^{\infty} {}^2\hat{b}_{-n} z_3^{-n} = {}^1\hat{\beta}(z_3) + {}^2\hat{\beta}(z_3^{-1})
\end{aligned} \tag{I2.32}$$

results into two series ${}^i\hat{\beta}(z_3)$, that meet the convergence requirements of Theorem I2.1 or Corollary I2.1. Hence, the transformation by means of (I2.10) in Corollary I2.2, results in two functions ${}^1\beta(z_3)$ and ${}^2\beta(z_3^{-1})$ that are recursively stable, if recursed in the appropriate direction; ${}^1\beta(z_3)$ in the positive and ${}^2\beta(z_3^{-1})$ in the negative z_3-direction. From (I2.30) and I2.32) it is verified that

$${}^2\beta(z_3^{-1}) = {}^1\beta(z_3)\big|_{z_3 = z_3^{-1}} = {}^1\beta(z_3^{-1}). \tag{I2.33}$$

Form the product

$$\tilde{\beta}_{0,0}(z_3) = {}^1\beta(z_3)\,{}^2\beta(z_3^{-1}). \tag{I2.34}$$

Since,

$${}^1\hat{\beta}(z_3) = \ln[{}^1\beta(z_3)] \tag{I2.35a}$$

$${}^2\hat{\beta}(z_3^{-1}) = \ln[{}^2\beta(z_3^{-1})] \tag{I2.35b}$$

and

$${}^1\hat{\beta}(\omega_3) + {}^2\hat{\beta}(-\omega_3) = \hat{\beta}_{0,0}(\omega_3) = \ln\{\beta_{0,0}(\omega_3)\} \tag{I2.35c}$$

the frequency responses of $\tilde{\beta}_{0,0}(\omega_3)$ and $\beta_{0,0}(\omega_3)$ are identical. Therefore, the replacement of $\beta_{0,0}(z_3)$ by $\tilde{\beta}_{0,0}(z_3)$ does not affect the frequency response of $H(z_1, z_2, z_3)$.

It is understood that, $\tilde{\beta}_{0,0}(z_3)$ is recursively stable iff it is implemented such a way that, each ${}^i\beta(z_3)$ recurses in the appropriae direction. Furthermore, $1/\tilde{\beta}_{0,0}(z_3)$ can be implemented as [6]

$$\frac{1}{\tilde{\beta}_{0,0}(z_3)} = \frac{1}{{}^1\beta(z_3)} T \frac{1}{{}^1\beta(z_3)} T \tag{I2.36}$$

where $T(\cdot)$ is a data inversion in z_3-direction. Under this implementation,

$$\tilde{\beta}_{0,0}(z_3) \neq 0, \qquad \text{for } |z_3| \leq 1. \tag{I2.37}$$

Hence, stability condition (I2.20c) is satisfied, and the filter $H(z_1, z_2, z_3)$ is stable.

Truncation Considerations

Having formulated the cepstrum of $\tilde{\beta}_{0,0}(z_3)$ by means of (I2.32), the coefficients of the recursively stable functions

${}^i\beta(z_3)$ are determined by using (I2.10):

$$ {}^ib_0 = e^{i\hat{b}_0}$$

$$ {}^ib_p = \sum_{m=1}^{p} \left(\frac{m}{p}\right) i\hat{b}_m\, {}^ib_{p-m}, \qquad \text{for } p \neq 0.$$

If the method developed is to be numerically implemented, each series must be truncated to $\{{}^ib_p\}_0^{\pm M_i}$. (Recall that for $i=1$, $p \geq 0$, whereas for $i=2$, $p \leq 0$.) This truncation may affect the stability of $\tilde{\beta}_{0,0}(z_3)$. The following theorem assures that there are finite numbers M_i, that result into stable truncated functions $\tilde{\beta}_{0,0}(z_3)$.

Theorem I2.4 [10]

Suppose the recursively stable power series:

$$\beta(z_3) = \sum_{m=0}^{\infty} b_m z_3^m.$$

The series $\{b_m\}_0^{\infty}$ is absolutely convergent and

$$|\beta(z_3)| > 0, \qquad \text{for } |z_3| \leq 1.$$

The absolute convergence of $\{b_m\}$ guarantees that there exist a number M such that

$$|\bar{b}(z_3)| = \left| \sum_{m=0}^{M_1} b_m z_3^m \right| > 0$$

for every $M_1 \geq M$ and $|z_1| \leq 1$.

This theorem guarantees the existence of a pair (M_1, M_2) such that the power series

$${}^1\beta(z_3) = \sum_{m=0}^{M_1} {}^1b_m z_3^m$$

$${}^2\beta(z_3^{-1}) = \sum_{m=0}^{M_2} {}^2b_{-m} z_3^{-m}$$

and, consequently,

$$\tilde{\beta}_{0,0}(z_3) = {}^1\beta(z_3)\,{}^2\beta(z_3^{-1})$$

(under the appropriate recursion scheme), are recursively stable.

To find a first constraint on the truncation parameters M_1 and M_2, consider the arrays $\{{}^1b_n\}$ and $\{{}^2b_{-n}\}$ with length (M_1+1) and (M_2+1) correspondingly. The array of their cascade $\tilde{\beta}_{0,0}$ is of length (M_1+M_2+1), whereas the array of the original function $\beta_{0,0}$ is of length $(2NI+1)$. Therefore, if the array $\tilde{\beta}_{0,0}$ is to be at least as large as $\beta_{0,0}$, the following condition must be imposed.

$$M_1 + M_2 \geq 2NI.$$

For arrays such as $\tilde{\beta}_{0,0}$, which is symmetric with respect to $m=0$, an appropriate choice is

$$M_1 = M_2 = NI.$$

The particular choice $M_1 = M_2 = NI$, may give satisfactory results in terms of stability.

Appendix II

Theorem II.1

The cascade of two rotated filters, one rotated over an angle $\beta = 225°$ and the other over an angle $\beta + 90° = 315°$, possesses quadrantal symmetry in its magnitude response.

Proof:

The magnitude of the 1-D transfer function $H(s)$, is centrally symmetric:

$$|H(s)| = |H(-s)|. \tag{II.1}$$

The transfer function (in s-domain) of the first filter, rotated over an angle β, is

$$H_2^1(s_1, s_2) = H(s_2\cos(\beta) - s_1\sin(\beta))$$

$$= H\left(-\frac{\sqrt{2}}{2}(s_2 - s_1)\right). \tag{II.2}$$

The transfer function of the second one, rotated over $\beta + 90°$, is

$$H_2^2(s_1, s_2) = H(s_2\sin(\beta) + s_1\cos(\beta))$$

$$= H\left(\frac{\sqrt{2}}{2}(s_2 + s_1)\right). \tag{II.3}$$

Define $F_2^1(s_1, s_2)$, $F_2^2(s_1, s_2)$ and $F_2(s_1, s_2)$, the magnitude response of the first, the second filter and their cascade, correspondingly. From (II.1), (II.2), and (II.3)

$$F_2^1(s_1, s_2) = F_2^2(s_1, -s_2) \tag{II.4}$$

and

$$F_2^1(s_1, s_2) = F_2^1(-s_1, -s_2) = F_2^1(s_2, s_1). \tag{II.5}$$

Using (II.1), (II.4), and (II.5), the following relations can be easily proved:

$$\begin{aligned} F_2(s_1, s_2) &= F_2^1(s_1, s_2)F_2^1(s_1, -s_2) = F_2(-s_1, s_2) \\ &= F_2^1(-s_1, s_2)F_2^1(-s_1, -s_2) = F_2(s_1, -s_2) \\ &= F_2^1(s_1, -s_2)F_2^1(s_1, s_2) = F_2(s_2, s_1) \\ &= F_2^1(s_2, s_1)F_2^1(s_2, -s_1). \end{aligned} \tag{II.6}$$

Since $(-s)$ corresponds to (z^{-1}), by the bilinear transformation $s_i = (1-z_i)/(1+z_i)$, (II.6) is equivalent to

$$F_2(\omega_1, \omega_2) = F_2(-\omega_1, \omega_2) = F_2(\omega_1, -\omega_2) = F_2(\omega_2, \omega_1) \tag{II.7}$$

References

[1] M. E. Zervakis and A. N. Venetsanopoulos, "Three-dimensional digital filters using transformations," in *Applied Digital Filtering; Adaptive and Nonadaptive*, Ed. M. H. Hamza, Acta Press, pp. 148–151, June 1985.

[2] K. Hirano, M. Sakane, and M. Z. Mulk, "Design of three-dimensional recursive digital filters," *IEEE Trans. Circuits Syst.*, vol. CAS-31, pp. 550–561, June 1984.

[3] I. Pitas and A. N. Venetsanopoulos, "The use of symmetries in the design of multidimensional digital filters," *IEEE Trans. Circuits Syst.*, vol. CAS-33, pp. 863–873, Sept. 1986.

[4] J. J. Murray, "A design of method for two-dimensional recursive digital filters," *IEEE Trans. Acoust., Speech, Signal Processing*, vol. ASSP-30, pp. 45–51, Feb. 1982.

[5] J. M. Costa and A. N. Venetsanopoulos, "Design of circularly symmetric two-dimensional recursive filters," *IEEE Trans. Acoust. Speech, Signal Processing*, vol. ASSP-22, pp. 432–442, Dec. 1974.

[6] J. M. Costa and A. N. Venetsanopoulos, "A group of linear spectral transformations for two-dimensional digital filters," *IEEE Trans. Acoust., Speech, Signal Processing*, vol. ASSP-24, pp. 424–425, Oct. 1976.

[7] T. F. Quatieri and D. E. Dudgeon, "Implementation of 2-D digital filters by iterative methods," *IEEE Trans. Acoust., Speech, Signal Processing*, vol. ASSP-30, pp. 473–487, June 1982.

[8] M. Zervakis, "Design of 3-D digital filters using transformations," M.A.Sc. thesis, Univ. of Toronto, Ont., Canada, 1985.

[9] B. D. Anderson and E. I. Jury, "Stability of multidimensional digital filters," *IEEE Trans. Circuits Syst.*, vol. CAS-21, pp. 300–304, Mar. 1974.
[10] P. Pistor, "Stability criterion for recursive filters," *IBM J. Res. Develop.*, pp. 59–71, Jan. 1974.
[11] S. G. Tzafestas, *Multidimensional Systems. Techniques and Applications*. New York: Marcel Dekker, 1986.
[12] M. E. Zervakis and A. N. Venetsanopoulos, "Design of three-dimensional rotated infinite impulse response digital filters," *Signal Processing*, pp. 30, in press.
[13] P. Agathoklis, and L. T. Bruton, "Practical BIBO stability of *n*-dimensional discrete systems," *Proc. Inst. Elect. Eng.*, vol. 130, pt.G, no. 6, Dec. 1983.
[14] G. V. Mentonca, A. Antoniou, and A. N. Venetsanopoulos, "Design of two-dimensional rotated digital filters satisfying prescribed specifications," *IEEE Trans. Circuits Syst.*, vol. CAS-34, pp. 1–10, Jan. 1987.

M. E. Zervakis was born in Crete, Hellas in 1961. He received the Diploma of Engineering from the University of Sallonica, Hellas, in 1983, and the M.A.Sc. from the University of Toronto, in 1985, all in electrical engineering. He is now working towards the Ph.D. degree in electrical engineering at the University of Toronto, Toronto, Ont., Canada.

His interests are in multidimensional signal processing and pattern recognition using fuzzy set theory.

Mr. Zervakis is a Scholar of the Public Benefit Foundation, "Alexander S. Onassis," and a member of the Technical Chamber of Hellas.

✠

Anastasios N. Venetsanopoulos (S'66–M'69–SM'79), for a photograph and biography please see page 10 of the January 1987 issue of this TRANSACTIONS.